EVALUATION OF GEOMORPHIC PROXIES FROM HIGH RESOLUTION TOPOGRAPHIC DEMs IN OBLIQUE SUBDUCTION ZONES: WESTERN PUERTO RICO

By

INÉS MARÍA BARRIOS GALÍNDEZ

Bachelor of Civil Engineering

Universidad de Carabobo

Valencia, Carabobo- Venezuela

2007

Submitted to the Faculty of the
Graduate College of the
Oklahoma State University
in partial fulfillment of
the requirements for
the Degree of
MASTER OF SCIENCE
May, 2018

EVALUATION OF GEOMORPHIC PROXIES FROM HIGH RESOLUTION TOPOGRAPHIC DEMs IN OBLIQUE SUBDUCTION ZONES: WESTERN PUERTO RICO

Thesis Approved:

Dr. Daniel Laó –Dávila

Thesis Adviser

Dr. Mohamed Abdelsalam

Dr. Javier Vilcáez

ACKNOWLEDGEMENTS

I would like to thank my advisor Dr. Daniel Laó-Dávila for his patience, advice, guidance, and suggestions during this investigation. I am grateful to Dr. Mohamed Abdelsalam for his trust, motivation, good mood, his always welcoming attitude, and for always believing in our work. Thank you to Liang Xue for the time dedicated to help me processing the proxies and for introducing me and teaching me about the method. Thank you to the suggestions and time of my committee. I am thankful to Open Topography and UNAVCO in Boulder Colorado, for sponsoring the LiDAR training. Thank you to Martin Isemburg for offering with no cost his Lasstool software for research. Lastool was utilized to start the processing of LiDAR images. Thank you to Chesapeake Foundation scholarship and Martin Family Foundation for partially support my Master Degree. I am thankful to Boone Pickens School of Geology the professors, students and staff, who make this school a diverse and inclusive family from all around the world.

Thank you to my tectonic research group; it has been an honor to learn with all of you and share the most intellectually stimulating conversations. Special gratitude to my friend and lab mate Luelseged Emishaw who is being a mentor on understanding geologic process and offering me his friendship during my time in OSU. My appreciation and sincere friendship to Micah Mayle, for his everyday support and always have the willingness to help solve any data or software problem.

Thank you to Steven Johnson and Folarin Kolawole who dedicated time and effort to understand the Caribbean tectonics and offer suggestion about my research. I also want to thank Andrew Katumwehe and Kat Roberson for helping me in the early stages of this research. I am also grateful to all the fellow graduate students from the Oklahoma School of Geology.

Infinite gratitude and recognition to my beloved husband Christopher Gammon always believing in me, for your support, patience, and edits in my research. Your love, care, encouragement and comprehension have been vital to keep me motivated and happy to achieve this goal. Thank you to my mother her infinite love and absolute dedication. Thank you for always having the right word to keep me motivated and thank you for being such a great role model in my academic formation. Thanks to my father, for your love and support and for staying by our side while I achieve my goals. Thanks to my sister for staying supportive of our parents while I complete this task. Special thanks to the daily support of my best friend and life sister Maylin Melo, who is being there for me every day during this journey. Lastly I want to thank my Latinas friends in Tulsa, the family who received me in this country and the people that have given me a home in Oklahoma.

Name: Inés María Barrios-Galíndez

Date of Degree: MAY 2018

Title of Study: EVALUATION OF GEOMORPHIC PROXIES FROM HIGH RESOLUTION TOPOGRAPHIC DEMs IN OBLIQUE SUBDUCTION ZONES: WESTERN PUERTO RICO

Major Field: Geology

Abstract:

We examined geomorphic proxies in oblique subduction zones with very low tectonic uplift rate using western Puerto Rico as case study. The Puerto Rico and the Virgin Island microplate is located at the NE corner of the Caribbean plate oblique subduction boundary with the North America plate. Seismic hazard is a major concern in the region, due to the frequent medium to low activity in the island. Active faulting has been suggested specially in the western part of the island, but limited research has been done about location and mechanisms of the faults. Geomorphic proxies have been recognized to be useful to estimate parameters like spatial and temporal distribution of rock uplift, and to assess the maturity and stability of drainage basins. Nevertheless, geomorphic proxies have been mainly tested in collisional margins with high uplift rates and rift settings with moderate uplift rates. This work aims to test three independent geomorphic proxies, Chi integral (X), Asymmetric Factor (AF) and Normalized Steepness (Ksn) in western Puerto Rico to compare them with passive seismic data and lineament analysis using digital elevation model (DEM) from LiDAR, SRTM and NED data. Our goals with this work are (1) Test the usefulness of geomorphic proxies in subduction zones with low uplift rates (2) Identify surface lineaments in southwestern Puerto Rico that could be indicative of faulting (3) Correlate this information with the distribution pattern of the geomorphic proxies, to identify faults that could be active or reactivated. Performing geomorphic proxies analysis in Puerto Rico provided significant results in subduction zones with very low tectonic uplift. In addition our results provide some insight of the displacement of faults in south Boquerón Bay, La Parguera, Punta Montalva, Guánica and Cerro Goden fault. It also suggest possible reactivation of faults in South Boquerón Bay, Sierra Bermeja, La Parguera, Guánica, San Germán Fault, La Torre fault and Cerro Goden Fault.

TABLE OF CONTENTS

Chapter Page

LIST OF FIGURES

Figure Page

CHAPTER I

INTRODUCTION

Geomorphic proxies are numerical models from topography data (DEMs) to simulate current geometrical configuration of river networks. River networks record the geomorphic responses to tectonics and climatic changes that control the channels morphology and gradient (Perez-Peña et al., 2010; Kirby and Whipple, 2012). Various geomorphic proxies have been developed based on the analysis of these responses, in distinct geologic sites to model tectonic settings, structural features, climatic and lithological controls.

Geomorphic proxies, like Chi integral (χ), Asymmetric Factor (AF) and Normalized Steepness (Ksn), provide insights on the spatial and temporal patterns of rock uplift (Kirby and Whipple, 2012), fault activity (Xue et al., 2017), fault linkage (Cowie et al., 2006), and rapid crustal deformation (Chen et al., 2003). This information of deformation and faulting is important to develop more accurate seismic and tsunami hazard programs. While in tectonics, it help us to understand the interaction and mechanisms of plate boundaries.

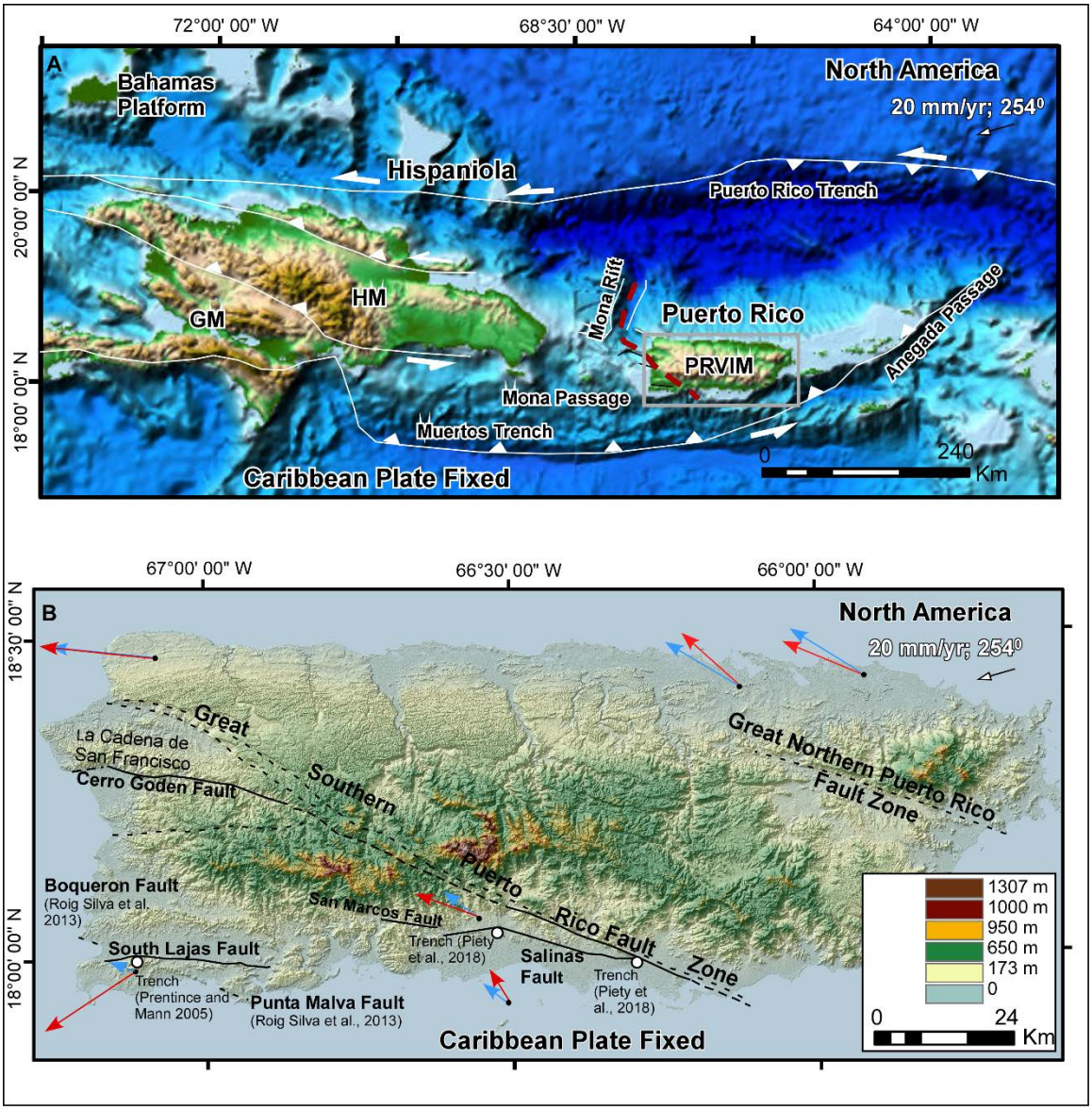

Fig 1. A. Tectonic map of the northeastern North America-Caribbean plate boundary zone. Gonave Microplate (GM), Hispaniola Microplate (HM), and Puerto Rico Virgin Islands Microplate (PRVIM). Red line indicates projection of the Mona Rift on-shore (Laó-Dávila, 2014 modified from Wadge et al., 1984; Ryan et al., 2009). Map from ETOPO1, a global relief model of Earth's surface that integrates land topography and ocean bathymetry. B. Hill shaded color map of Puerto Rico showing Quaternary active faults (Modified from Piety et al., 2018). Map constructed from Shuttle Radar Topography data 30x30 m spatial resolution. Red arrows are observed velocities and blue arrows are calculated velocities from GPS (vectors velocities from ten Brink and Lopez 2012). Rates and directions of subductions from ten Brink and Lopez 2012

Studies in the Himalayas (Kirby and Whipple, 2012), the Alps (Ferraris et al., 2012), and the East Africa Rift System (Xue et al., 2017) characterized sites with high (>0.5 mm/yr.) and medium (between 0.04 mm/yr and 0.5 cm/yr) tectonic uplift rates and

geomorphic patterns in compressional and extensional regimes. These studies demonstrate how geomorphic proxies can be a valuable tool to study active orogens and correlate them successfully with river system dynamics by integrating information about incision rates, erosional responses, drainage maturity, and differential uplift to lithospheric deformation (Kirby and Whipple, 2014).

Nevertheless, geomorphic proxies have been less explored in oblique subduction zones with low tectonic uplift rates (≤0.04 mm/yr.), like in the Caribbean and North America plate boundary. One of the studies in the margin applied geomorphic proxies in Hispaniola and Greater Antilles, then tried to relate geomorphic expressions to the current relative movement observed between the North America and Caribbean plate boundary. The Hispaniola study suggested that the margin contain different blocks under rotation, uplifting and tilting movements (Rodríguez and Escribano, 2017). Another study, in the Caribbean-North America boundary specifically in northeastern Puerto Rico suggested that tectonics exert the main control in the geomorphic pattern observed in the tropical streams in the area (Brocard et al., 2015).

Puerto Rico is an area with high onshore shallow seismicity activity (<25 km) not related to the seismicity associated to the subduction zone. At least 1750 onshore shallow earthquakes (2.5-4.5 M) have been recorded from 1987 to 2017 (Puerto Rico Seismic Network and Huerfano et al, 2005). In addition, a recent paleoseismic study in Salinas, southwestern Puerto Rico, recognizes evidence of two earthquakes with a magnitude greater than6 (Pietty et al., 2018). Many GPS (Jansma et al., 2000, Jansma and Mattioli, 2005 Calais et al., 2015) geophysical (Roig-Silva et al., 2013), geomorphological (Mann et al., 2005) and field studies (Piety et al., 2018) have been

perform to try to characterize the deformation in Puerto Rico. Despite, the efforts in characterizing geomorphic patterns in the Caribbean island and in the Caribbean-North American plate boundary, the basic question of how strain is being accommodated in the area in relation to oblique subduction remains poorly understood.

Oblique subduction is poorly understood in these settings because even when the geometry of the margin is suggestive of transform faults and thrusting, Puerto Rico geomorphic features indicate strike slip and extension (Hippolyte et al., 2005). Conversely, thrusting and strike slip is observed in the neighboring island of Hispaniola (Perez-Peña et al., 2010), to the west of Puerto Rico. Understanding that geomorphic proxies have been less explored in low tectonic uplift boundary and the discrepancy in geomorphic patterns between Puerto Rico and Hispaniola relative to the nature of tectonic boundary, we propose to study χ, AF, and Ksn geomorphic proxies in western Puerto Rico to test their usefulness in oblique subduction settings, and to provide insights on active faulting and strain accommodation in the plate boundary.

The geomorphic difference between Puerto Rico and Hispaniola have been addressed by previous studies which have suggested that Puerto Rico is behaving as rigid microplate in which strain is accommodated offshore (Byrne 1985 et al., Masson and Scanlon, 1991; Jansma et al., 2000; Manaker et al., 2008; Symithe et al., 2000; Calais et al., 2015). Nevertheless, these studies do not account for the shallow seismic activity recorded in the area (Huérfano et al., 2005), and the geomorphic expressions suggestive of active faulting (Piety et al., 2018; Roig-Silva et al., 2013, Mann et al., 2005; Grindlay et al., 2005; Prentice and Mann et al., 2005).

For that reason, the offshore strain accommodation end member has been challenged by a group of researchers who hypothesized that strain was accommodating onshore after finding geomorphic surfaces suggestive of Quaternary active faulting. (Fig. 1A; Piety et al., 2018; Roig-Silva et al., 2013; ten brink and López-Venegas, 2012; Mann et al., 2005; Grindlay et al., 2005; Hippolyte et al., 2005; Prentice and Mann, 2005). For instance, Roig-Silva et al., (2013) characterized an active through-going left lateral fault system named Boquerón Bay-Punta Montalva fault zone in southwestern Puerto Rico (Fig 1B). Jansma and Mattioli (2005) suggested the Lajas Valley in the southwestern part of the island to be the focus of the highest permissible inland deformation (Fig 1B). Whereas, Mann (2005) suggested active faulting because of observed river deflections and displaced fans in the Cerro Goden Fault (Fig 1B).

Active faulting exploration in Puerto Rico still has many question to be answered such as localization of faults in areas with high shallow seismicity with obscured surface expressions, about permissible rates of displacements along the mapped faults and therefore the possible occurrence of larger earthquakes (Jansma and Mattioli, 2005). Some of the fault traces accounting for the concentration of earthquakes in the southwest present lack of continuity in their surface expressions along their inferred trace. South Lajas fault (Prentice and Mann et al., 2005) and Cerro Goden Fault (Mann et al., 2005) are examples of faults in which the characterization of the traces and displacements are not fully understood. Whereas, a more recent study reported two Holocene ruptures in Salinas, to the southeast of the Great Southern Puerto Rico Fault Zone (Piety et al., 2018). Furthermore, another important question to answer about Puerto

Rico geomorphology is why the current basin and range topography is suggestive of extension in an oblique subduction margins.

For this research, we used a combination of three proxies χ, AF, and Ksn with data about lithology, precipitation, climate and seismic events to correlate them with information about active faulting proposed in previous studies in Western Puerto Rico. To achieve these objectives, we evaluated χ, AF, Ksn in ten areas of western Puerto Rico, south Boquerón Bay, Sierra Bermeja, la Parguera, Punta Montalva, Guánica, north Boquerón Bay, Sierra de Guanajibo, northeastern Lajas valley, western Cerro Goden Fault, and Eastern Cerro Goden Fault. The analysis was performed by extracting geomorphic proxies from moderate-high resolution topography (10 x10 m) Lidar derived DEM to later correlate the values obtained and pattern of geomorphic proxies with final detail geology, with the purpose of finding areas of active tectonic uplift. These types of studies are significant because we can advance the techniques to constrain the areas of active faulting to later perform paleoseismic studies in reduced areas. With the ultimate goal to delineate obscured fault traces and measure their displacement and contribute to define areas with high seismic hazards.

CHAPTER II

LITERATURE REVIEW

Geomorphic indexes and their results

Numerical modeling, as geomorphic proxies, has been widely used to study tectonic geomorphology to understand landscape evolution (e.g. Dominguez-González et al., 2014, Xue et al., 2018), spatial and temporal uplift related to active faulting (Xue et al., 2018), and fault interaction and linkage (Cowie et al., 2006). Some examples of how proxies have been used in different setting with their important outcomes are given below.

To develop the χ proxy, drainage basin maturity was studied in three different tectonic settings (Willet et al., 2014). This study characterized the Loess Plateau as being close to equilibrium after finding the values of χ across the water divides were nearly equal. The east of central Taiwan to the contrary, is characterized as a young and tectonically active mountain belt because the values of χ across the water divides were very different. Whereas, southeastern United States also was suggested to be in disequilibrium also because the values of χ across water divides were distinct. To investigate uplift distribution in the eastern Tibetan Plateau, normalized steepness index was estimated and compared with lithology (Kirby and Whipple et al., 2003). This study

revealed that the lithology and steepness in this area had limited correlation, suggesting that the anomalies in the values of steepness estimates by the proxy distribution was related to uplift.

Localization of active faulting in south Taranaki, New Zealand was explored using AF proxy and a combination of other four proxies, stream length-gradient, stream gradient sinuosity and hypsometry. Fault traces and tectonically active areas were pinpointed with this study (Ries, 2013).

Geomorphic evolution of the Jamaican restraining bend in the Caribbean and North America plate boundary was also modeled after the application of hypsometric integral, normalized steepness, knick points and stream length gradient proxies (Dominguez-González et al., 2014). Some of the significant outcomes of this research was the identification of three distinct morphotectonic regions, each of them with a distinct geomorphic signature. They were also able to relate the distribution of uplift distribution with different structures.

The evolution and growth of the Ethiopia Plateau since 30 Ma was also analyzed using a combination of geomorphic proxies, like normalized steepness, hypsometric integral and chi integral (Xue et al., 2018). The proxies were compared with estimations of thickness of basalt and complemented with development of knickpoint celerity models. The spatial distribution of geomorphic proxies in the southern Main Ethiopian Plateau suggested a more tectonically active southeastern escarpment and three uplift events during the geologic history of the Plateau.

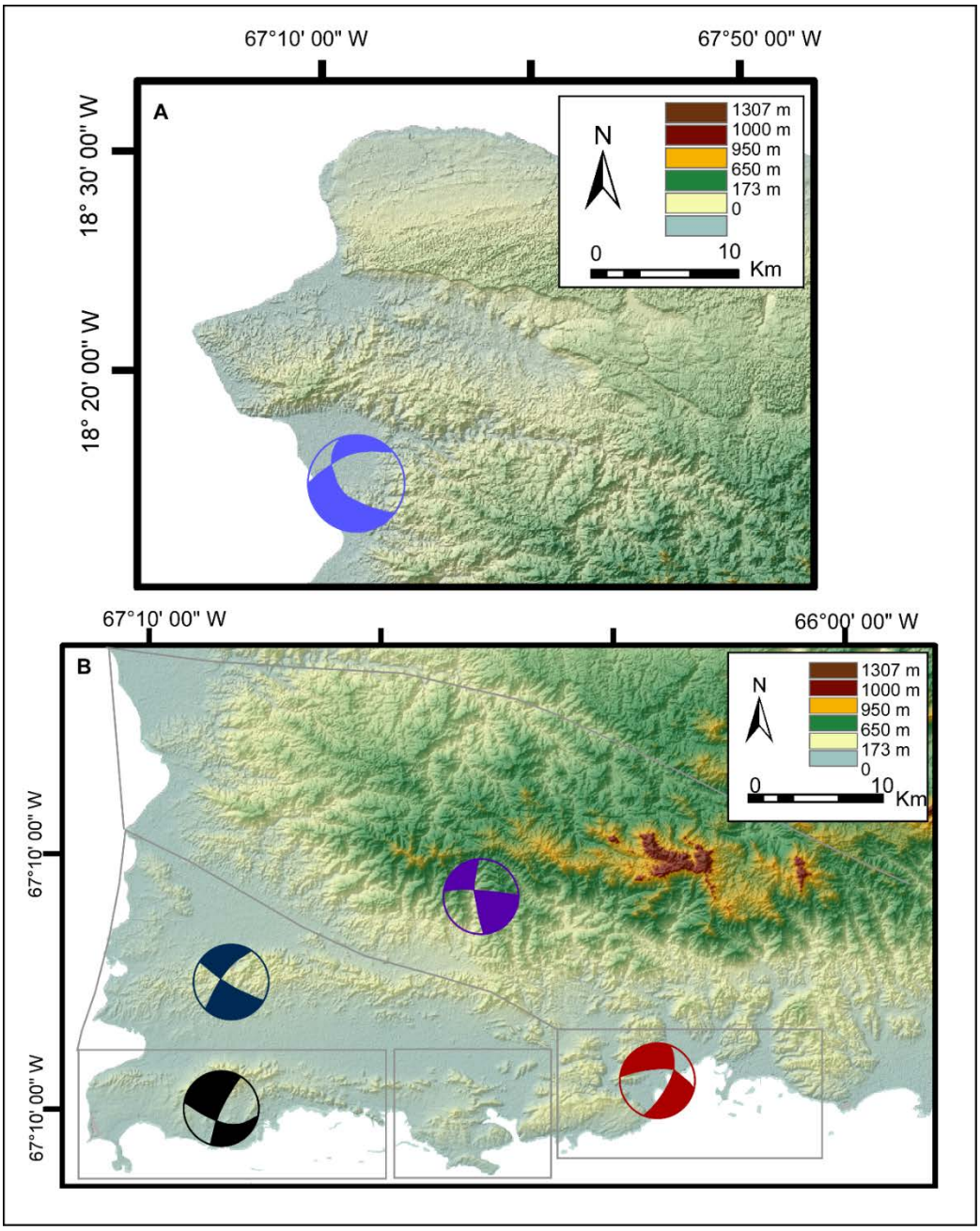

Fig 2. A. Focal Mechanisms from microseismicity of regions in the Cerro Goden Fault suggest oblique extension. Colors in focal mechanisms indicate different regions (Huérfano et al., 2005). B. Focal Mechanisms from microseismicity of regions in the Cerro Goden Fault suggest strike-slip movement. Colors in focal mechanisms indicate different regions (Huérfano et al., 2005).

Faults in western Puerto Rico

The Lajas valley and Lajas fault

The Lajas Valley is a linear basin of 30 km long and 1.5 to 4.5 km width in southwestern Puerto Rico (Mann et al., 2005). The valley strikes east-west and it is bounded by Sierra the Guanajibo to the north and Sierra Bermeja range and La Parguera and Punta Montalva hills to the south. River networks flowing on these mountain ranges are small and intermittent and feed water bodies and a large mangrove swamp in the Boquerón Bay.

The valley's linear geomorphology, bounded by approximately linear mountain ranges, its mostly closed interior drainage, and the high density of seismic events (Huérfano et al., 2005) suggest that active faulting has produced a graben that is controlling the shape of the valley (Mann et al., 2005, Grindlay et al., 2005). Holocene faulting may be related to the deformation in the Mona Passage as suggested by offshore and onshore studies (Mann et al., 2005, Grindlay et al., 2005; Roig Silva et al., 2013). Moreover, east-west striking serpentinites belts in the mountain ranges have shown spatial correlation with offshore Holocene ruptures in the Mona Rift, indicating possible reactivation of these faults.

The South Lajas fault was recognized from aerial photography and paleoseismic studies (Prentice and Mann 2005). Information obtained from the excavation defined two zones of faulting separated about 1 m, cutting the alluvium of eastern South Boquerón Bay. The fault has 1km long and a 1.5-3 m high differential elevation. Nevertheless, the fault was inferred to continue along the valley.

La Parguera hills

Earlier field studies in this area where not able to identify a fault in the area (Mattson 1960). Nevertheless, he reported the beds of the northern limb of the anticline overturned and the need of existence of a fault to correlate the structure to the beds located to the north (Mattson 1960). Later studies considered the thrust fault nonexistent because paleontological and stratigraphic evidence (Almy 1969) and recent research suggest no evidence of recent uplift in La Parguera (Mann et al., 2005).

North Boquerón Bay

The North Boquerón fault has been described as the last section of a compound fault system, which start with Punta Montalva fault going through Parguera and Sierra Bermeja in the northwest direction. Cutting through the alluvial deposits in the Lajas Valley and the Boquerón Mangrove Forest until the North Boquerón Bay fault section (Roig-Silva et al., 2013). Along the Punta Montalva-North Boquerón-Bay fault the strain was been suggested to be accommodated in bedrock, cutting across deformed Miocene limestone, shifting alluvial streams and alluvial deposits (Roig-Silva et al., 2013). The slip of the fault was suggested to be left-lateral strike slip (Roig-Silva et al., 2013).

San Germán Fault

San Germán fault was characterized to have a strike slip component and thrusting component (Volckmann 1984b; Laó-Dávila 2012). Thrusting of the serpentine chert and Yauco Formation are upon the Sabana Grande Formation (Volckmann 1984b,

Laó-Dávila et al., 2012). The age of these fault have been suggested to be older than middle Eocene (Laó-Dávila et al., 2012).

La Torre Fault

This fault was defined as a thrust fault, with the Sabana Grande and Yauco formations underthrusting the main serpentinites body and with a very irregular trace (Llerandi-Román, 2004; Laó-Dávila et al., 2012 and Slodowski et al., 1956). The Torre thrust was related with the relative displacement of San Germán fault. Later, the Torre fault was further characterized to strike NW to SE and dips of 45° to 66° (Laó-Dávila and Anderson, 2009). Dating of the Torre fault was reported as post-middle Eocene (Slodowski et al. 1956).

Cerro Goden Fault

The surrounding area of the range and Cerro Goden Fault have been described as heavily affected by tectonic and erosional control features, with north-dipping Oligocene to early Pliocene scarps of carbonate platforms facing southward (Mann et al., 2005). The Cerro Goden fault zone was located about 500 m south of La Cadena de San Francisco with a 15 km-long trace (Fig. 1B; Mann et al., 2005). The fault was described as having three distinct morphological sections based on aerial photographs, topographic maps, and satellite images (Mann et al., 2005). The northwestern part of the fault was reported as a straight fault separating the Cretaceous rocks of Rio Blanco Formation and the Rio Yauco Formation (McIntyre, 1971 and Mann et al., 2005). The central part of the fault was described to continue the west-northwest trending direction to the western part of Central La Plata quadrangle with a sharp

curvilinear edge separating the Eocene Culebrinas Formation and the Cretaceous Yauco Formation (McIntyre, 1971 and Mann et al., 2005). The western section of the fault was described as having an east-west striking direction, which separates the Añasco Valley bedrocks from the coast (Mann et al., 2005). The Cerro Goden fault was related to Quaternary geomorphic features like stream deflection, offset terrace raisers, mountain facing scarps, located to the central and eastward sections of the fault (Mann et al., 2005). The sense of motion of Cerro Goden Fault was proposed to be right-lateral after geomorphic expression of river deflection. This movement represents a younger slip with opposite sense than its original Late Eocene left-lateral movement (Laó-Dávila, 2014).

GPS velocities and displacements within western Puerto Rico

Comparison of differential GPS velocities of onshore vs offshore and onshore vs onshore stations has intended to constrain possible displacements along potentially active faults onshore Puerto Rico, like South Puerto Rico Fault zone, Cerro Goden Fault and within the Lajas valley in western Puerto Rico (Jansma and Mattioli, 2005). The permissible displacement of Southern Puerto Rico and Cerro Goden was measured in NS direction is been estimated to be less than 0.00-1.6 mm/yr. Whereas the velocity across the southwestern region of the island was suggested to be $\leq$ 2mm/yr of shortening, suggesting oblique reverse motion in the faults bounding the Lajas Valley (Jansma and Mattioli, 2005).

To the contrary, later studies suggested extension in SW Puerto Rico. Due to differential velocity between the GPS station located in the SW of the island moving in SW direction relative to the Caribbean Plate (the same direction than GPS velocities

measured in Hispaniola), while the rest of the GPS station within the island are moving in NW direction (Fig. 1B; ten Brink and López-Venegas, 2012). These differential velocities suggested 2-3 mm/yr. NW-SE extension in western Puerto Rico traced the possible margin of the Hispaniola and Puerto Rico Virgin Island microplate within Puerto Rico (Fig. 1B; ten Brink and López-Venegas, 2012).

Puerto Rico and Virgin Island neotectonics

Oblique subduction is been suggested to control the tectonics of the PRVIM since the late Eocene (Fig. 1A; Mann et al., 1998; DeMets et al., 2000; McCann et al., 2002; Prentice et al., 2003; Jansma and Mattioli, 2005). Nevertheless, there is also evidence of compressional and extensional features in the Puerto Rico Trench, Muertos Trough, Anegada Passage, and Mona Rift (Sykes et al., 1982; Mann and Burke et al., 1984; Burke et al., 1984; Byrne et al., 1985; Stein et al. 1988; Masson and Scanlon, 1991; Jansma and Mattioli, 2005; Grindlay et al., 2005; Hippolyte et al., 2005).

Three microplates have been identified in the northern Caribbean margin: the Hispaniola Microplate (HM; Byrne et al., 1985; Fig.1A), the Gonave Microplate (GM Mann et al., 1995), and the Puerto Rico and Virgin Island Microplate (PRVIM; Masson and Scanlon., 1991; Fig 1A). The microplate model assumes that the strain produced by the interaction between the North America and the Caribbean plates is being accommodated offshore. The microplate model suggest that PRVIM moves coupled to the Caribbean Plate while the Hispaniola Microplate is suggested to move independently from the Caribbean Plate due to collision with the Bahamas Platform (Calais et al., 2015; Fig 2A). This differential velocity, observed between the Hispaniola Microplate and the

PRVIM, suggests opening in the Mona Passage to the west of Puerto Rico (Calais et al., 2015; Fig. 2A). Conversely, an independent translation model reveal motion of the Puerto Rico plate with respect to the Caribbean (Jansma et al. 2000). These studies, raise an ongoing debate between the Puerto Rico Virgin Island (PRVI) rigid microplate model and the PRVI internal strain microplate model.

The Caribbean plate velocity respect to North America was estimated to be 19.4 ± 1.2 mm/yr toward $N79^0 \pm 3^0E$ (Jansma et al., 2000). Whereas, PRVIM have been suggested to move 2.6 ± 2.0 mm/yr toward N82° ±3.4 mm/yr relative to North America as computed from western Puerto Rico (Jansma et al., 2000). In addition, differential motion with the adjacent Hispaniola Microplate was recorded to be accommodated by slow (5 mm/yr.) rifting in the Mona Passage (Mann, 2005).

Seismicity in western Puerto Rico.

The PRSN recorded 828 earthquakes between 1987 and 2002 in western Puerto Rico (Huérfano et al., 2005). There are records of at least four destructive earthquakes since 1700 (Motazedian and Atkinson 2005). In addition, there are registers of a 7.3 M earthquake in 1918 (McCann1985, 2002) and a possible great earthquake in 1787 (Motazedian and Atkinson 2005). High concentration of shallow seismicity <30 km is registered south of the Southern Puerto Rico Fault Zone which have been related to interplate deformation (Fig 1: Huérfano et al., 2005). While intermediate depth seismicity is linked to the Caribbean plate motion corresponding to the north dipping slab in the Muertos Trough, with depths over 25 km (Huérfano et al., 2005). Deeper earthquakes were recorded by Ascencio et al., (1980) in a diffuse south dipping zone beneath Puerto

Rico which extends up to a maximum depth of 155 km. Shallow earthquakes have been reported to be located around the belts of serpentinites in southwest Puerto Rico. In addition, some concentrations of earthquakes are associated to the major fault systems in the island, the Southern Puerto Rico Fault zone and the Northern Puerto Rico Fault Zone (Fig. 1B; Huérfano et al., 2005).

Geology of western Puerto Rico

Puerto Rico has Late Jurassic to early Tertiary volcanic, volcaniclastic, metamorphic, and sedimentary rocks (Mattson, 1960; Mattson and Pessagno 1979, Monroe 1980). Researchers divided the geology of Puerto Rico into three geographic provinces separated by the major fault zones: the Northeastern, Central and Western Provinces (Jolly et al., 1998; Glover, 1971; Mattson, 1979). The Southern Puerto Rico Fault Zone separates the Western Province from the Central province. While the Northern Puerto Rico Fault Zone separates the Central and the Northeastern provinces (Jolly et al., 1998; Glover 1971; Mattson 1979). The geology of the Western Province is classified into three principal regions from the southwest to the northeast. (1) A pre-arc complex of ultramafic rocks, associated pelagic sediment, and altered mid-ocean ridge basalt. (2) Two isolated domains in the southwest of volcanic and sedimentary strata with Campanian serpentinized peridotite in the central part of the province. (3) Dominantly pyroclastic accumulation from the Campanian to Eocene with flanking deltaic fan deposits (Jolly et al. 1998).

Sierra Bermeja is an 8 km long ophiolitic mélange striking east-west in southwestern Puerto Rico which contains the oldest rocks in the island (Mattson 1960,

Laó Dávila 2014). This complex contains the Jurassic Mariquita Chert (Mattson 1979). Younger cherts within the Mariquita Chert of the Bermeja Complex contain tuff layers, suggesting the ocean floor received pyroclastic deposits as it approached the island arc (Mattson and Pessagno, 1979). The overlying island arc sequence is a 1-3 km long andesitic flow intrusion and volcanic clastic deposits interlayered with shallow water platform carbonates (Larue et al., 1991). Post volcanic sedimentary deposits together with coastal recent deposits cover areas in the north and the south of the island from Oligocene and younger (Monroe, 1976).

CHAPTER III

METODOLOGY

Remote Sensing.

Remote sensing techniques were used to map the surface structures and to compare structural information of active faulting in western Puerto Rico available from previous studies. The three types of remote sensing data used were (1) Shuttle Radar Topography Mission (SRTM) Digital Elevation Model (DEM), 30 meters spatial resolution from the NASA; available from the Consortium for Spatial Information (CGIAR-CSI SRTM 90m Database), (Fig. 2), (2) Light Detection and Ranging (LiDAR), 10 m spatial resolution available from the National Oceanic and Atmospheric Administration (NOAA), and (3) National Elevation Data (NED) in 10m spatial resolution.

The study area is highly vegetated and usually cloudy, which can be a problem to map with remote sensing techniques. I used available SRTM-DEM and LiDAR images that subtract the effect of both vegetation and cloud cover.

Shuttle Radar Topography and Digital Elevation Models

DEMs were created using hill-shade technique from SRTM data. Hill-shaded maps were constructed with 30 m x 30 m spatial resolution. Lineaments were mapped as part of the structural analysis.

In addition, the DEMs were used to find stream deflections in the areas where lineaments were identified. Stream deflection is a morphological feature that indicates strike slip faulting (e.g. Mann et al., 2005; Roig-Silva et al. 2013). Stream deflection was verified with the satellite image in Google Earth. Active faulting will be determined by comparing the spatial relationship of the lineaments, streams deflection, and previously mapped faults.

Lidar and Digital Elevation Models.

LAStools Classification, Mosaicking and Format Transformation.

The LiDAR data for western Puerto Rico was acquired between January 10 and February 8 of 2004 by the U.S. Army Corps of Engineers. Some quality issues have been reported in the metadata file of this data set. For that reason, it was used by comparing it with the SRTM data NED (National Elevation Data) data and Google Earth satellite images. Areas with suspicious quality issues, such as artifacts, were not used in this study.

Air-borne LiDAR technology generates point clouds that sample the elevation of a terrain (Isemburg, 2016). To store and deliver the LiDAR data, the American Society of Photogrammetry (ASPRS) created a simple binary exchange in LAS format (LiDAR data exchange format; Isemburg, 2016). The LAS format records information specific to

the LiDAR data (return#, intensity value, xyz coordinates, etc.). Due to the amount of information, the LAS data format is provided in a compressed LAZ format and is delivered in tiles (Isemburg, 2006).

To create the western Puerto Rico DEM from LiDAR, 95 tiles in LAZ compression format were downloaded and processed. Each tile covers approximately 4 x 4 km^2 of area. Each of the tiles are subsequently decompressed, classified, mosaicked, and converted into tiff format using LAStool software.

The BLAST tool was used to process of high-density point clouds into raster files in tiff format, and to classify the points. Through the classification, the points corresponding to vegetation were discarded. In addition, the BLAST tool was used to mosaic the 95 files into one raster. From the raster in tiff format, the DEM models were constructed. The LIDAR 2004 data is available with classified points but LAStool was used to mosaic and convert the file from LAZ format to tiff format.

LiDAR

LiDAR records and allows detailed measurements of fault zones (Arrowsmith and Zielke, 2009). LiDAR airborne laser swath mapping (ASLM), with 10 m x 10 m resolution, was used in the areas of previously suggested active faulting and correlated this information with SRTM DEM and satellite images from Google Earth. The higher resolution of the LiDAR allowed us to see details in geomorphology and in the fault zones to perform a detailed lineament analysis

Studies of landforms in geomorphology tectonics have demonstrated to be significant because they allow correlating strain release measurements using geologic data in million-year time scale and GPS data in decadal time scale (Arrowsmith and

Zielke, 2009). Combining landforms as indicators of movement along and across the fault zone with Quaternary geochronology have been essential to develop later studies on fluid flow along fault zones, fault zone strength, evolution of fault zone fabrics and even to indicate places to do excavation of trenches (Arrowsmith and Zielke, 2009). Using LiDAR 1 m x1 m to do geomorphology investigation have been lately very useful in places like San Andreas faults in California to characterized fault zones for different reasons. One of the most important reasons is because the data offers accurate fine scale measurements of small features recorded by earthquakes on the surface (Arrowsmith and Zielke, 2009).

The detailed mapping achieved using LiDAR have been compared with the one obtained by geologist in the field, with the advantage of being able to cover the extent of the fault zone (Hudnut et al., 2002). LiDAR acquisition is usually gathered by scanning (10-100khtz) pulse of near infrared for terrestrial LiDAR and visible for bathymetry (Donellan et al., 2015).

Geomorphic proxies**:**

Morphotectonic analysis was performed in ten areas of western Puerto Rico (Fig. 3). Five areas located to the south of the Lajas Valley: south Boquerón Bay, Sierra Bermeja, Parguera, Punta Montalva, and Guánica. Three areas to the north of Lajas Valley: North Boquerón Bay, mountain range from Lajas to Sabana Grande, and northeastern Lajas. Lastly, two areas along La Cadena of San Francisco, northwestern

Cerro Goden Fault, and northeastern Cerro Goden Fault. To compute geomorphic proxies, we used LiDAR and NED raster DEMs with 10 m^2 resolution.

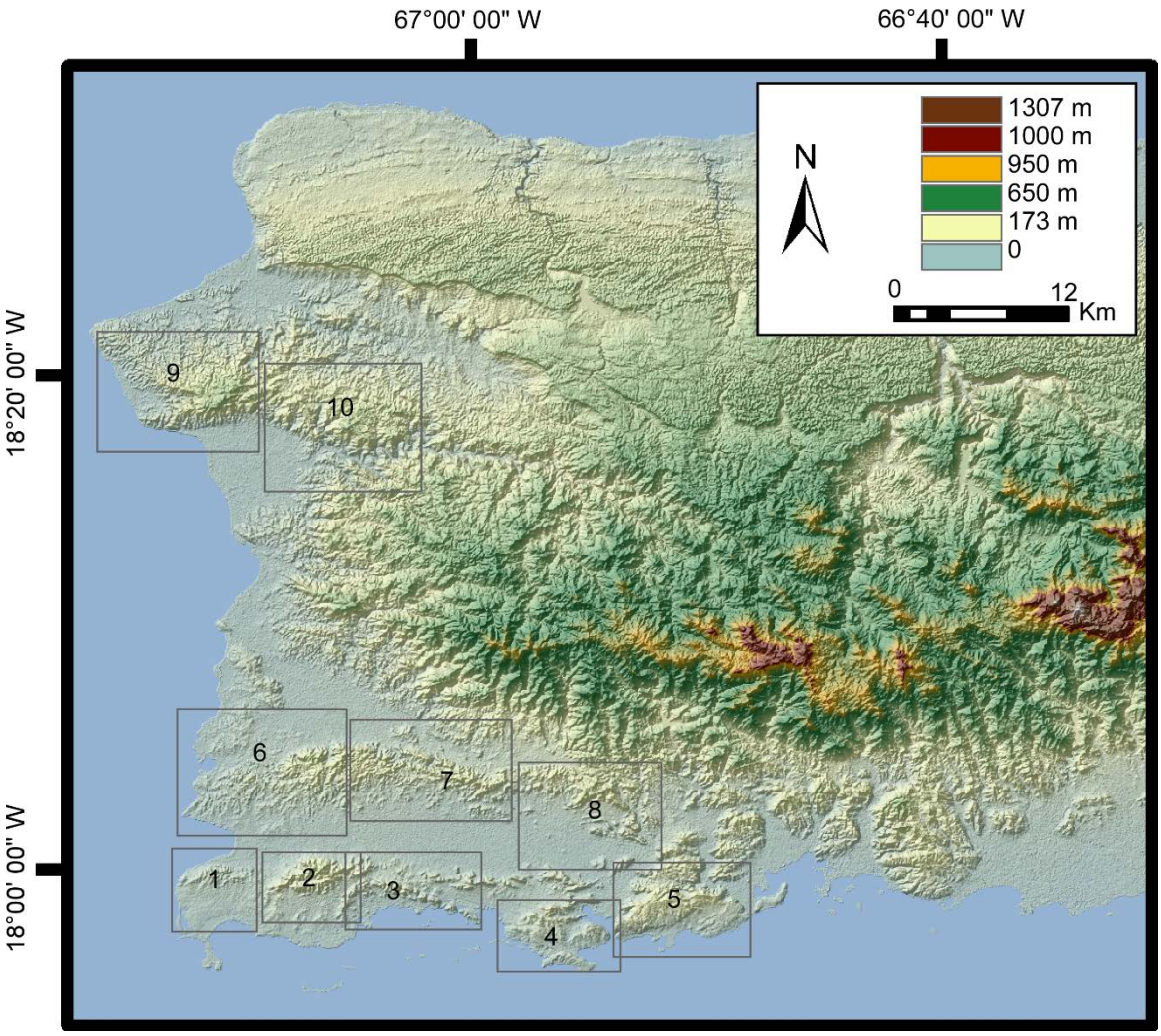

Fig 3. SRTM DEM showing study areas in western Puerto Rico: 1) South Boquerón Bay, 2) Sierra Bermeja, 3) La Parguera, 4) Punta Montalva, 5) Guánica, 6) North Boquerón Bay, 7) The Sierra de Guanajibo, 8) North Eastern Lajas 9) Western Cerro Goden Fault and 10) Eastern Cerro Goden Fault.

We used areal proxies and linear proxies. The areal proxies performed include Asymmetric Factor (AF) and it is often used to evaluate the basin's maturity and the stage of equilibrium of the basin (Perez-Peña et al., 2010). Areal proxies describe the general characteristics of the basin including basin's extent, shape, and relief. Within the

linear geomorphic proxies, we evaluated Chi integral (χ) and normalized steepness (Ksn). Linear proxies are computed from stream's profiles, using Topo Toolbox from ArcGIS. Linear proxies have been suggested to be a representative of local erosion and rock uplift in previous studies (Montgomery and Brandon, 2002; Wobus et al., 2006; Kirby and Whipple 2012).

Chi analysis (χ).

Chi analysis is a model for the river basin dynamics in the present geometry configuration, which is based on steady state river channel (Willett et al., 2014). Chi estimates elevation for a stream location considering it is in steady state (Willett et al., 2014). River basins evolve by lateral migration of drainage divides because of differential erosion on opposite sides of the divides (Willett et al., 2014). This relationship between erosion and river incision is expressed by the stream power law, which proposed that erosion in bedrock rivers is proportional to the power the river spends on its bed (Howard et al., 1994; Willett et al., 2014). Therefore, erosion can be calculated from drainage area and the channel slope with this formula $E = KA^mS^n$ (Perron and Royden, 2013, Mudd et al., 2014). Where S is the local gradient, A is the basin's drainage area, m and n are empirical constants. Assuming topographic steady state ($\partial z/\partial x = 0$) with uniform topographic uplift (E) and erosion rate (K), stream power model can be also expressed as

$$S = \frac{\partial z}{\partial x} = \left(\frac{E}{K}\right)^{1/n} \mathrm{A}^{m/n} \qquad (1)$$

Where z is the elevation of the stream and x is the longitudinal coordinate (distance from the head of the stream to the location along the longitudinal profile at a z value). Solving the equation by integrating both sides of the equation

$$z(x) = z(x_b) + (\frac{E}{KA_0{}^m})^{\frac{1}{n}}\chi \quad (2)$$

Where $z(x_b)$ is the elevation at the mouth of the drainage basin and A_0 is the reference drainage area (Perron and Royden, 2013)

$$\chi = \int_{x_b}^{x} (\frac{A_0}{A(x)})^{\frac{m}{n}}\, dx \quad (3)$$

$$\chi = (\frac{E}{KA_0{}^m})^{\frac{1}{n}} \quad (4)$$

The parameter χ gives information about the river system topology and geometry, suggesting how tectonic forces generates changes in topography throughout a river basin (Willet et al., 2014). Based on measuring disequilibrium of opposing river channels, Chi can be used to suggest the stability and motion of rivers drainage divides and the direction that would bring the contiguous channels toward equilibrium (Willet et al., 2014). The value of χ in equation (2) estimates the stream steady state at certain location (Willet et al., 2014). Consequently, variation in the values of χ along drainage divides, considering that rock uplift is constant, indicates motion of the divide from low to high χ values. Therefore, geometric equilibrium will produce a map with equal values across all water divides. While disequilibrium will result in drainage migration or river capture until equilibrium is reached. Planform view for disequilibrium state will show different values across the water divides (Willet et al., 2014).

For this study, χ was computed for DEMs derived from LiDAR and NED data covering all Puerto Rico. Nevertheless, this study is focused on western Puerto Rico. χ was calculated using TopoToolbox 2, a program of MATLAB developed to study DEMs (Schwanghart and Scherler, 2014).

Asymmetric Factor (AF)

Tectonics processes can be identified on the geomorphology of river networks, as stepping geomorphologies, gradient reduction or lateral tilting (Ries, 2013). Measuring tilting in river basins together with geomorphology studies can provide good indicatives of tectonics effects (Ries, 2013). River networks over homogeneous strata that have not been affected by tectonic movements are anticipated to show a dendritic and symmetric shape (Schumm et al., 2002). To the contrary, asymmetric river networks have been associated with recent tectonic activities (Schumm et al., 2002). When tilting of the catchment is parallel to the main trunk, migration of the streams in the direction of the tilting can be observed (Ries, 2013). The asymmetry of basins is analyzed by previously calculating the asymmetric factor, which is computed from the relationship between the area on one of the sides of the trunk stream and the area of the catchment. Asymmetric Factor is defined according to the following equation

$$AF=\frac{A_L}{A_t}-0.5$$

Where A_L is the area in the left of the trunk and A_T is total area of the basin. TopoToolbox in ArcGIS was used to generate catchment delineation and to calculate AF. Then, the basins' extent and half of the basins were manually delineated. The AF relationship's calculation was performed using ArcGIS.

The asymmetric factor of basins in western Puerto Rico was computed from NED data. The basins chosen to calculate the asymmetric factor were picked according to the following criteria, (1) Basins located in mountain ranges (because the basin delineation within ranges is more accurate). (2) Basins in which previous studies have shown active faulting (mountain ranges surrounding Lajas Valley and basins in Cerro Goden Fault). (3) Basins within the mountain ranges in which the Chi proxy showed anomalies indicatives of active faulting. According to the three criteria described, the study area was refined to three main ranges, (1) Ranges located to the south of Lajas valley (Sierra Bermeja, La Parguera hills, Punta Montalva hills and Guánica), (2) Sierra de Guanajibo range, (3) Range located north of the Cerro Goden Fault, La Cadena de San Francisco.

Normalized steepness (Ksn)

The normalized steepness (Ksn) index, according to the stream power-law, characterizes the channel's slope normalized to the upstream drainage contributing area and the difference between the area of reference. It can be calculated according to the following equation $Ksn = Ks\ A^{(Aref-A)}$, where Ks is the channel steepness, A is the contributing drainage area, and Aref is the area of reference. Relative high Ksn values within a region have been related with tectonic settings that experience fast tectonic uplift while relative low Ksn values within a region have been related with tectonic settings that have not experience tectonic uplift (Ismail and Abdelsalam, 2012).

The Ksn index is considered proportional to the river's incision rate derived by tectonic uplift, when keeping lithology and weather conditions homogeneous

(Whipple, 2004; Wobus et al, 2006; Ismail and Abdelsalam, 2012). To evaluate the influence of lithology and climate in this tectonic setting we analyzed the probability distribution function to Ksn, χ and, AF. In addition, we compared the different climate patterns in the north and the south with the rates of erosion obtained. Normalized steepness was also estimated using the TopoToolbox and using DEMs from NED.

Study areas

To evaluate the three proxies in western Puerto Rico, we divided the analysis per proxies for the 10 study areas (Fig. 3). In southwestern Puerto Rico we evaluated the mountain ranges located to the north and to the south of the Lajas Valley. They were divided in eight areas, South Boquerón Bay, Sierra Bermeja, La Parguera, Punta Montalva, Guánica, North Boquerón Bay, Sierra de Guanajibo range and NE Lajas valley. While in northwestern Puerto Rico the mountain ranges studied were located along the previously proposed Cerro Goden Fault. Bellow we will describe the obtained results from χ, AF, and Ksn proxies for each area.

CHAPTER IV

RESULTS

Chi integral (χ):

High values of χ show disequilibrium and migration of the drainage divides from low to high values. Areas mapped in orange (Fig. 4 and Fig. 5) represent high values of χ while areas mapped in green represent low values of χ. In South Boquerón Bay, in the southwestern flank of Lajas Valley, high values of χ were found to the northwestern area of the mountain range (Fig.4A), with drainage divides moving to the southwest (Fig. 11D).

High values of χ in the Sierra Bermeja were found located on top of the going outward alluvial fans (Fig. 4B). For this location the pattern of migration does not follow a linear trend, instead, it seems to be moving from the center of the range outward (Fig. 12D).

In La Parguera hills, some artifacts are observed in the northeastern part of the region, but clear high values of χ were found in the central area of the Parguera hills (Fig. 4C). These high values indicate migration of the drainage divide to the northeast (Fig. 13D).

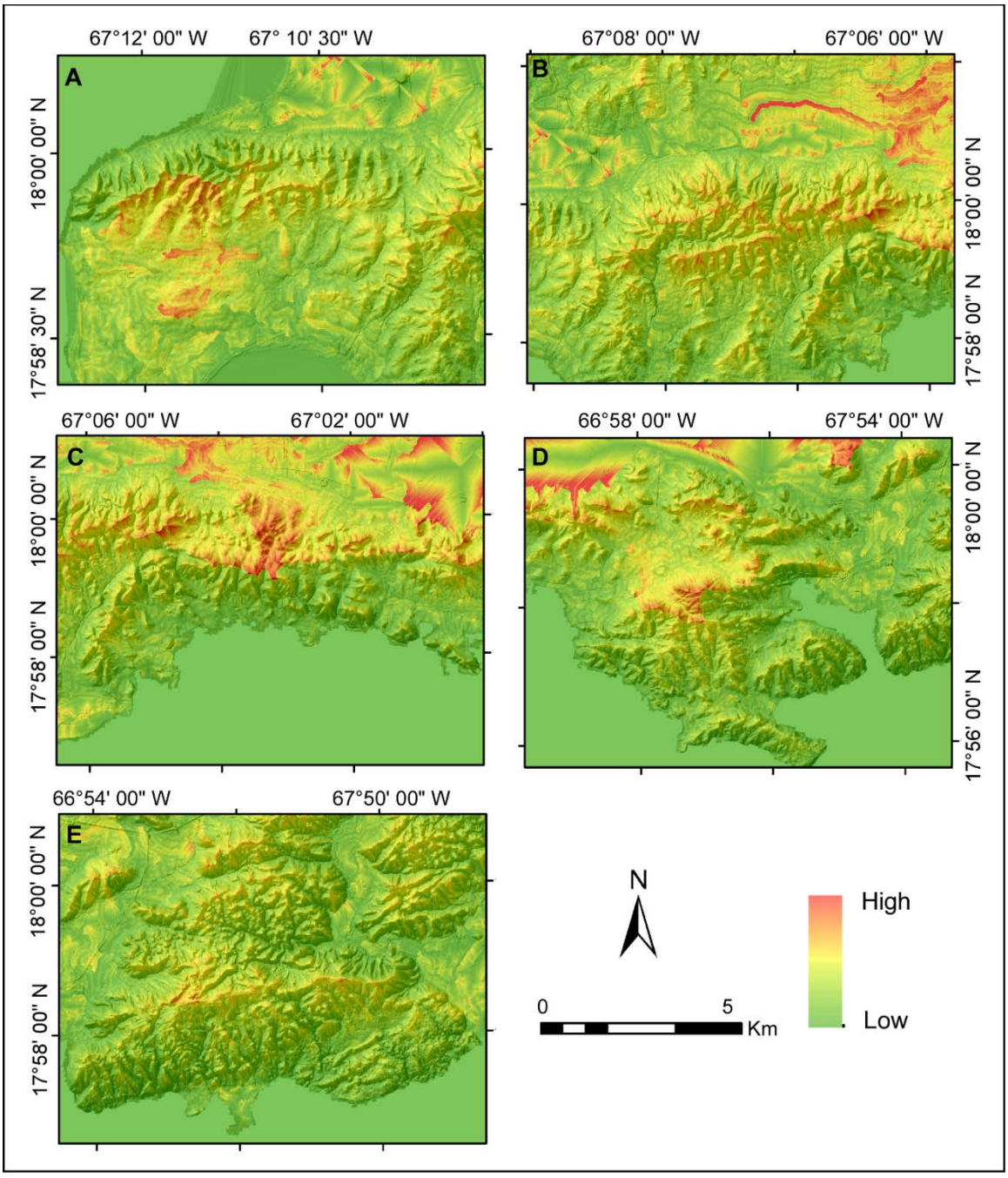

Fig 4. Chi integral for five areas of southwestern Puerto Rico. A. South Boquerón Bay (1); B. Sierra Bermeja (2); C. Parguera (3); D. Punta Montalva (4); E. Guánica (5). Numbers show areas in Fig 3.

In Punta Montalva, high values of χ are located in the central area of the mountain range, and some artifacts also appears in the northwest corner of the mapped area (Fig. 4D). Migration direction in Punta Montalva is to the southwest (Fig. 14D).

While in Guánica, slightly high values of χ were found close to the central part of the area in approximate east-west direction (Fig. 4E), with possible migration of the range to the north north-east direction (Fig. 15D).

North Boquerón Bay, shows significant high values of χ in the eastern area in study in the Sierra de Guanajibo (Fig. 5A). The Sierra de Guanajibo mountain range located in the northern border of Lajas valley between San Germán and Lajas, has distinctive high values of χ trending approximately east west direction of the study area (Fig. 5B) with scattered migration patterns (Fig 17D).

Northeastern Lajas Valley shows some artifacts located to the southwest but it also shows a clear pattern of high values of Chi in the northeast quadrant of the area (Fig.5C). Migration patterns are not well defined in this area (Fig. 18D).

In northwestern Puerto Rico along Cerro Goden Fault, high values of χ are scattered from west to east, along top of La Cadena de San Francisco (Fig. 5D and Fig. 5E). Western Cerro Goden Fault values are slightly elevated with migration patterns of the drainage divides to the northwest (Fig. 5D). While eastern Cerro Goden Fault values of χ are higher with migration patterns to the northeast (Fig. 5E).

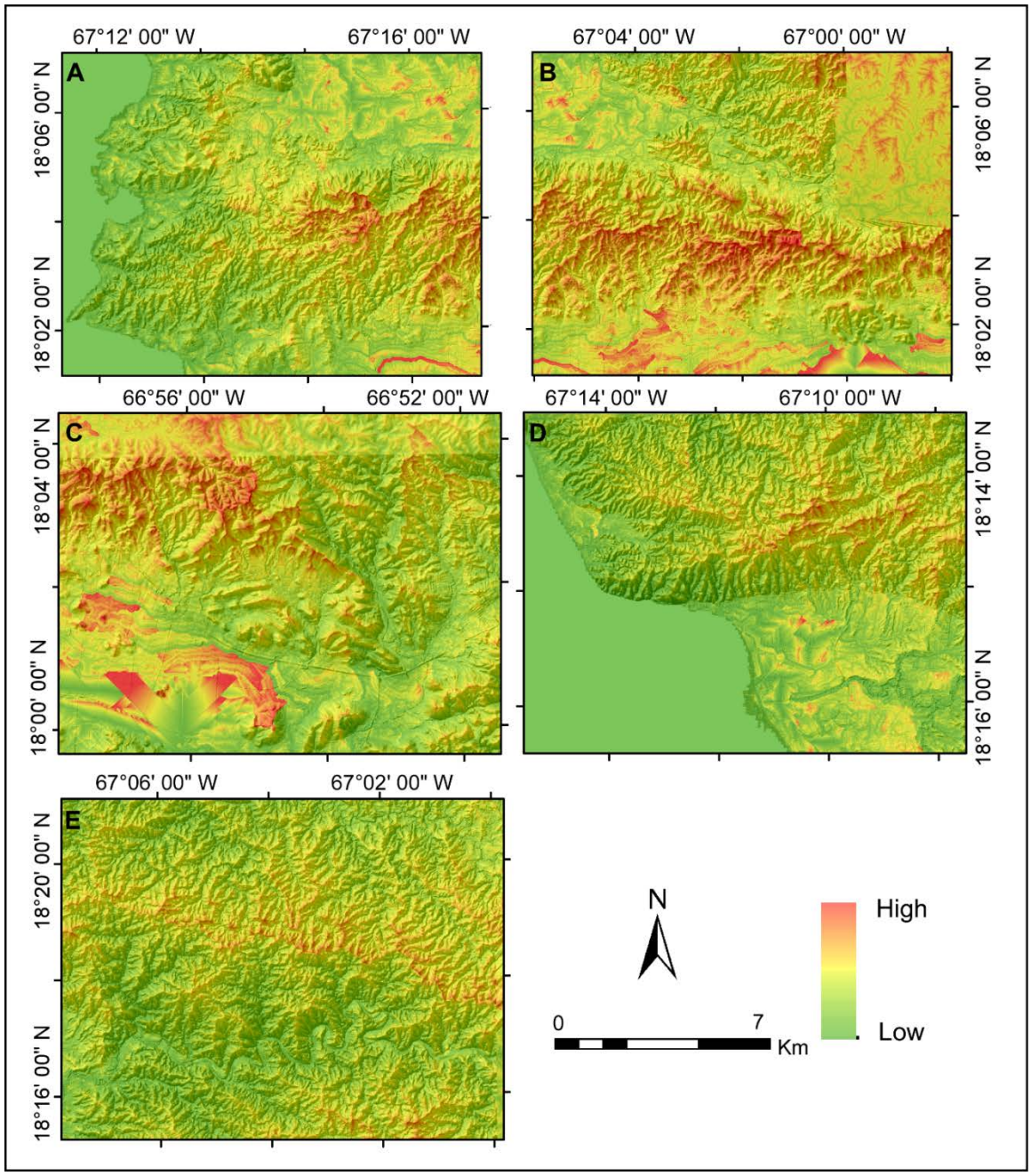

Fig 5. Chi integral for 3 areas north of Lajas Valley and along the Cerro Goden Fault in northwestern Puerto Rico, A. North Boquerón Bay/Cabo Rojo (6); B. The Sierra de Guanajibo (7); C. Northeastern Lajas (8); D. Western Cerro Goden Fault (9); E. Eastern Cerro Goden Fault (10). Numbers show areas in Fig 3.

Asymmetric Factor (AF):

The basins were divided into symmetrical when AF ≈ 0, moderately symmetrical between $\left|0.1\right|$ and $\left|0.2\right|$ and highly asymmetrical when AF values are > $\left|0.2\right|$. The AF values of South Boquerón Bay range between -0.09 and 0.169. Symmetrical basins in yellow are randomly located. Basins from 5-9 in orange form a trend of basin tilted to the east (Fig. 6A). In Sierra Bermeja AF values range between -0.15 and 0.279. Symmetrical basins are also randomly located. Basin 33 is highly tilted to the east and together with basins, 44-46, 50, 58, 64-66 indicate a trend of basins tilted to the east (Fig.6B).

In La Parguera, AF values range between -0.2809 and 0.2263. Symmetrical basins in yellow from 80 to 83 form a trend. Some asymmetrical basins in this area are randomly located indicating no trend (Fig.6C).

Punta Montalba AF vary from -0.09 to 0.18 and most of the basins in this area are asymmetrical and tilted to the southwest (Fig. 6D). Basins in Guánica are also mostly asymmetrical but no trend of tilting direction was found. AF values in Guánica range between -0.24 to the 0.21 and no tilt trend observed in this area (Fig. 6E).

In Northern Boquerón Bay, basins are also asymmetrical but tilted to southwest with AF values ranging between -0.35 to 0.16 and some symmetrical basins randomly located (Fig. 7A). The Sierra de Guanajibo range does not show a trend of symmetrical or asymmetrical basins and similar observation are shown in northeastern Lajas valley (Fig.7B and Fig. 7C).

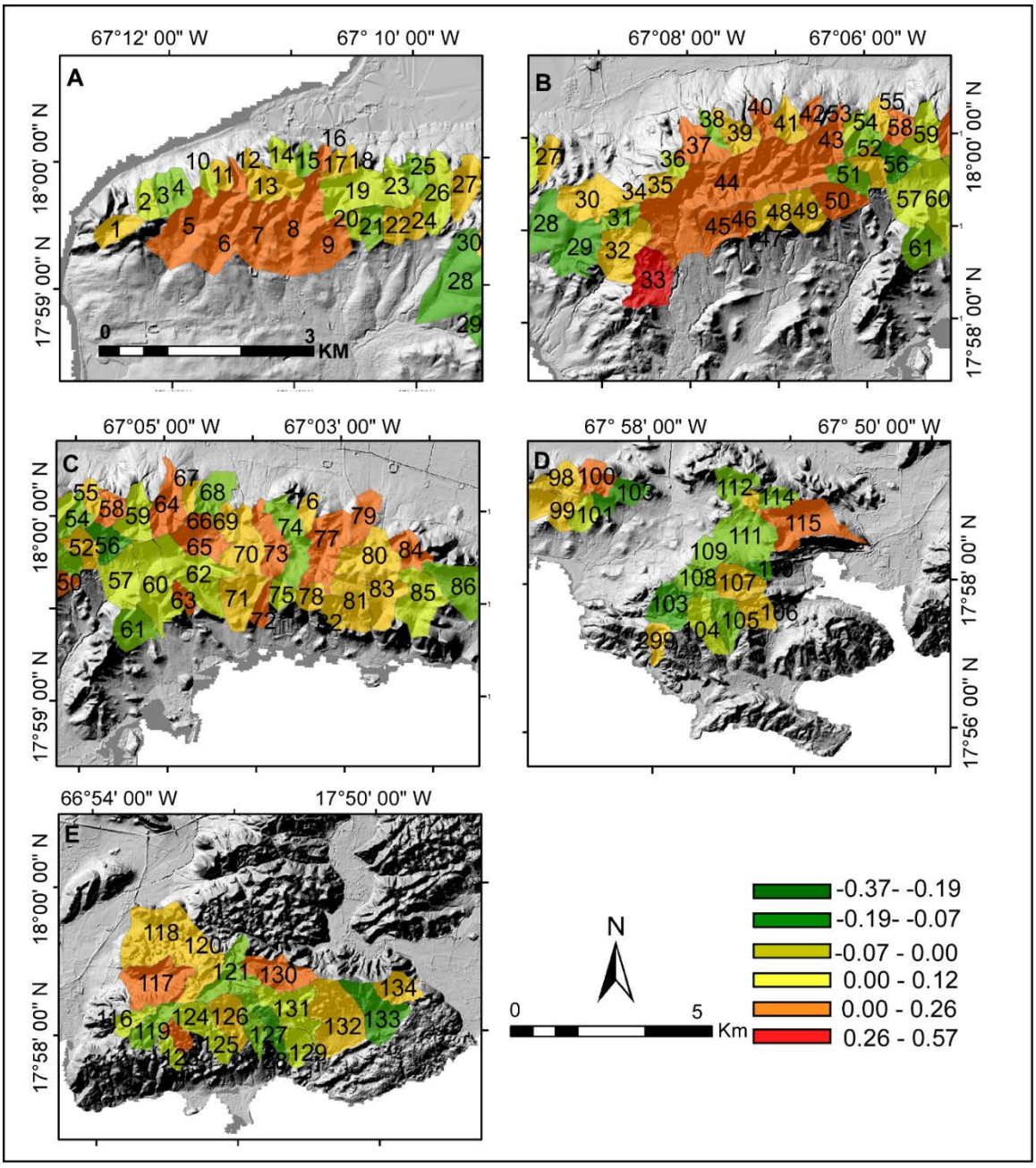

Fig 6. Asymmetric Factor in five areas of southwestern Puerto Rico, A. South Boquerón Bay(1); B. Sierra Bermeja (2); C. Parguera (3); D. Punta Montalva (4); E. Guánica (5). Numbers show areas in Fig 3.

Nevertheless, the mountain ranges located to the west (Fig. 7D) and east (Fig. 7E) within La Cadena de San Francisco, along Cerro Goden Fault, corresponding to the numbers 247 to 271 show a trend of asymmetrical basins tilted to the west with AF values ranging from -0.15 to 0.16.

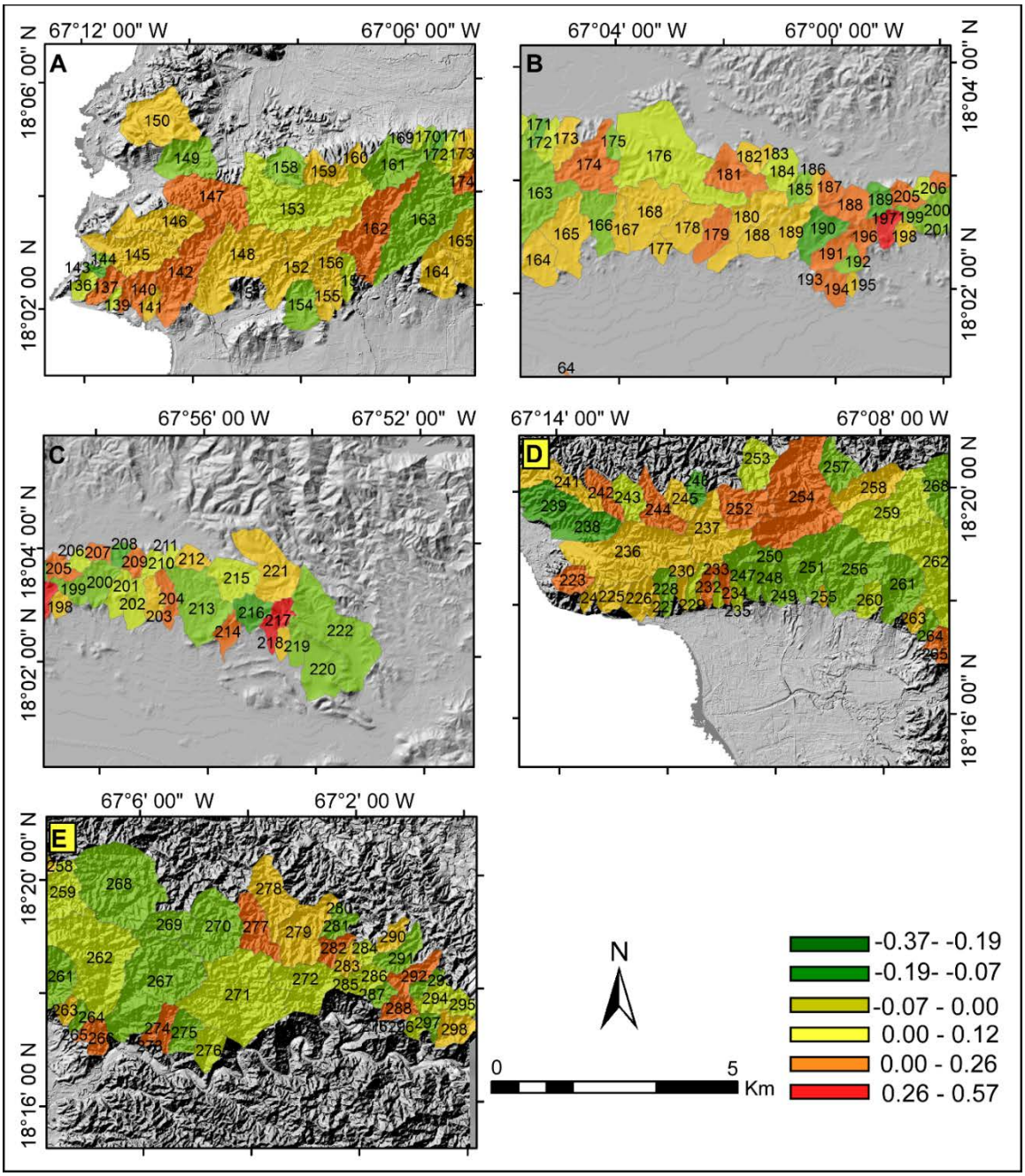

Fig 7. Asymmetric Factor in three areas north to Lajas Valley and along the Cerro Goden Fault in northwestern Puerto Rico, A. North Boquerón Bay/Cabo Rojo (6); B. Lajas-Sabana Grande (7); C. Northeastern Lajas (8); D. Western Cerro Goden Fault (9); E. Eastern Cerro Goden Fault (10). Numbers show areas in Fig 3.

Normalized steepness (Ksn)*:*

Normalized Steepness (Ksn) maps show high changes of erosion rates as indicated by color change in the maps. Southern Boquerón Bay shows slightly rate of changes of Ksn in the alluvial fan to the south of Lajas Valley (Fig. 8A). While in Sierra Bermeja rate of change of erosion is high and it is observed in the northern and southern flanks of the range (Fig. 8B). In La Parguera, the higher rates of change are located trending from northwest to southeast of the mapped area (Fig. 8C). In Punta Montalva, the rate of change of Ksn are not as significant (Fig. 8D). However, in Guánica high rates of Ksn change were found in the southwest costal area trending from southwest to the northwest (Fig. 8E).

In Northern Boquerón Bay, similarly to Punta Montalva the rate of change is not as noticeable as the other areas mentioned above (Fig 9A). Nevertheless, the Sierra de Guanajibo range show a change in Ksn (Fig. 9B and 9C). Significant Ksn rate of change was found along the Cerro La Cadena de San Francisco in the southern facing flank of the mountain range trending from west to east (Fig. 9D and 9E).

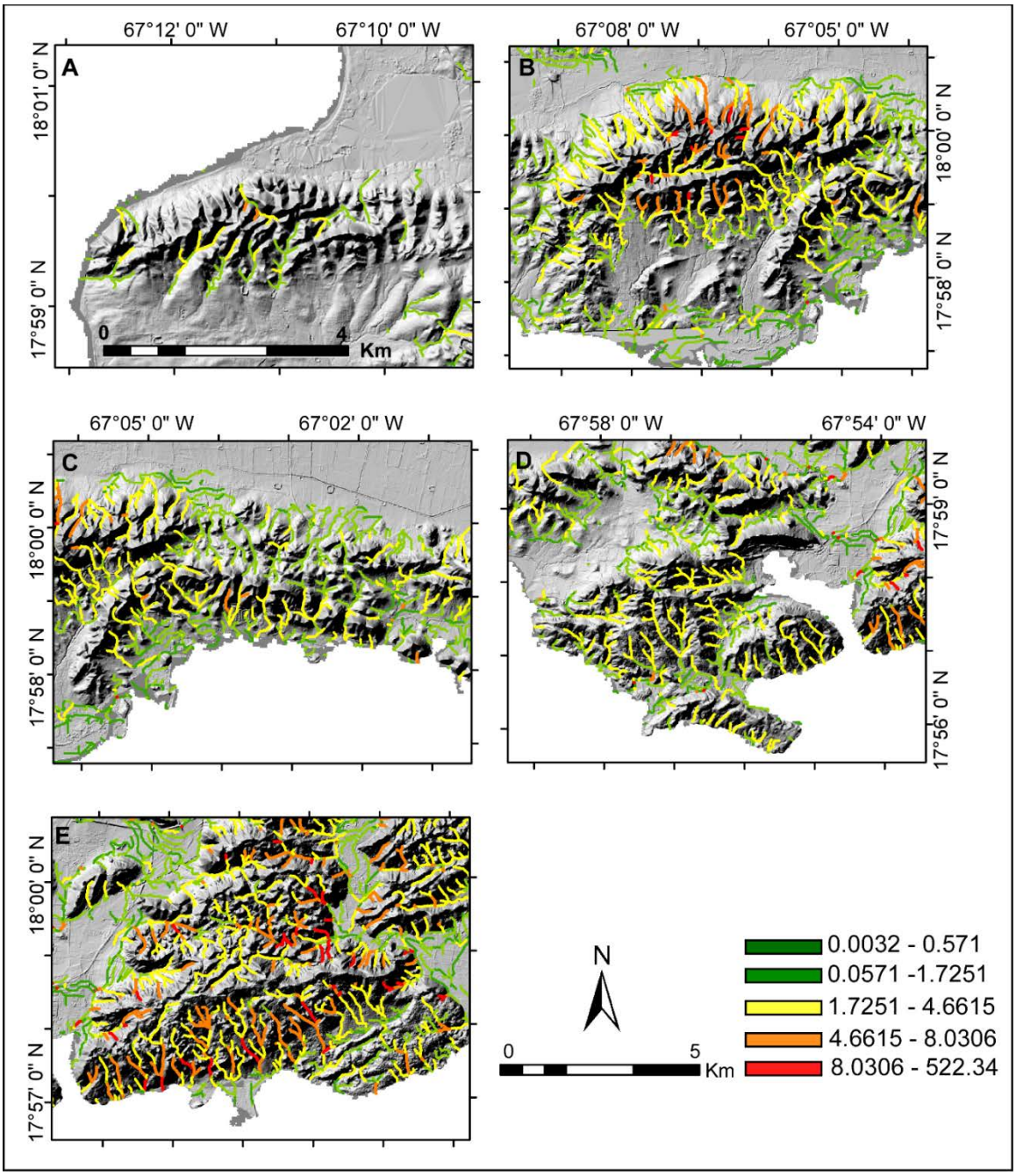

Fig 8. Normalized Steepness in in five areas of south western Puerto Rico, A. South Boquerón Bay (1); B. Sierra Bermeja (2); C. Parguera (3); D. Punta Montalva (4); E. Guánica (5). Numbers show areas in Fig 3.

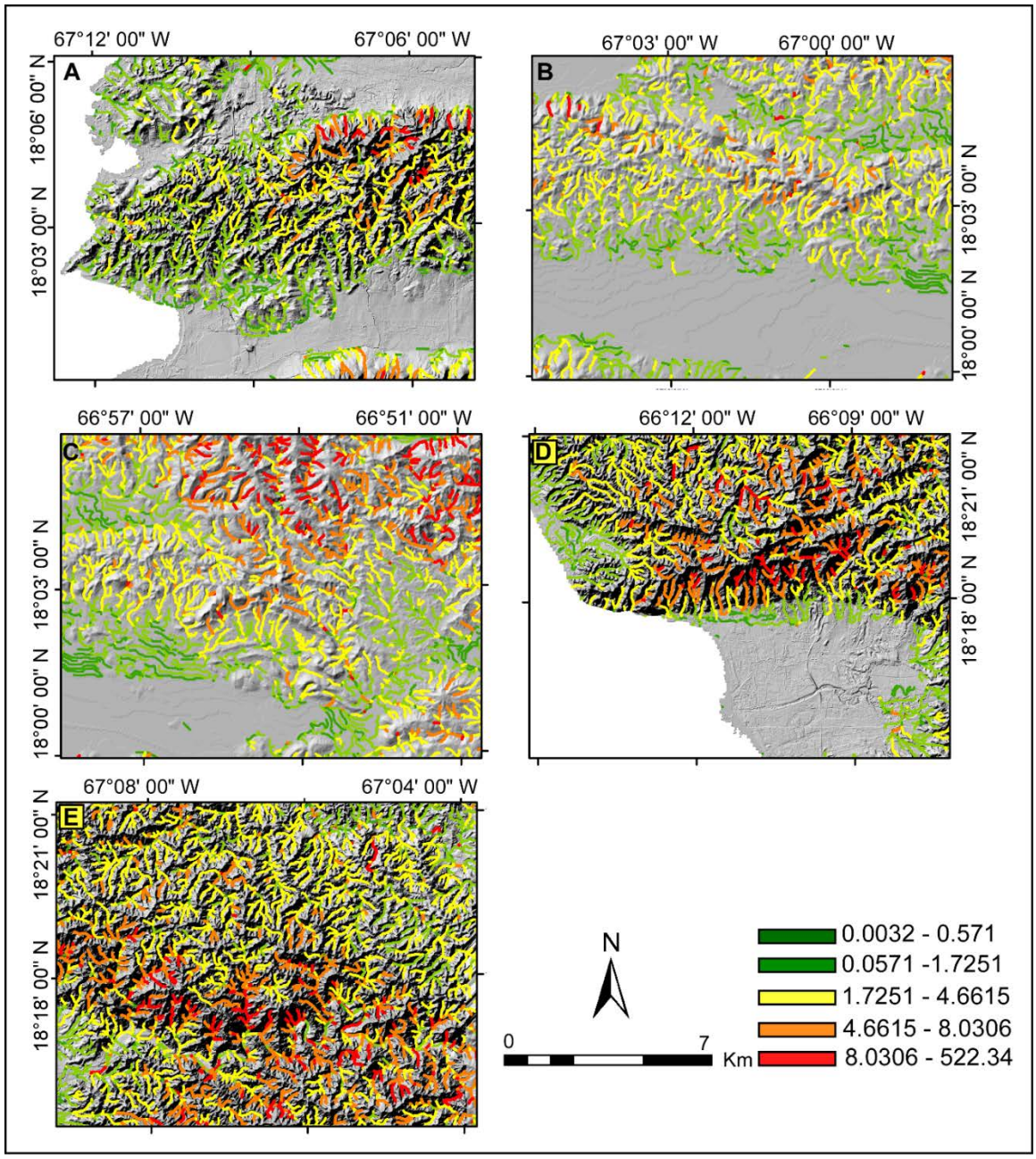

Fig 9. Normalized Steepness in three areas north to Lajas Valley and along the Cerro Goden Fault in northwestern Puerto Rico, A. North Boquerón Bay/Cabo Rojo (6); B. The Sierra de Guanajibo (7); C. Northeastern Lajas (8); D. Western Cerro Goden Fault (9); E. Eastern Cerro Goden Fault (10). Numbers show areas in Fig 3.

CHAPTER V

DISCUSSION

Evaluation of geomorphic proxies relative to lithology and precipitation

In this section, we discuss the possible influence of precipitation and lithology in the uplift patterns and erosion rates observed in the proxies. To assess the possible dependence of the three proxies χ, AF, and Ksn relative to the change of lithology, we calculated the probability distribution function (PDF) of each of the proxies per lithological unit in the study areas (Xue et al., 2018). We found that the signal recorded by the proxies does not show primary correlation with the lithological changes and the variation of rock strength and composition in western Puerto Rico (Fig. 10). To the contrary, the distribution of the PDF function shows similar and consistent distribution for the three proxies in six different lithological units (Fig. 10). The PDF was calculated in seven lithological Cretaceous to early Tertiary volcanic clastic rocks: Late Cretaceous limestone in southwestern Puerto Rico, Jurassic to Cretaceous serpentinite belts located in Sierra Bermeja and southeastern Monte del Estado, lower to upper Cretaceous basalt, Late Jurassic to early Cretaceous Marquita chert in Sierra Bermeja, and the Oligocene-Miocene sedimentary limestone in La Cadena de San Francisco.

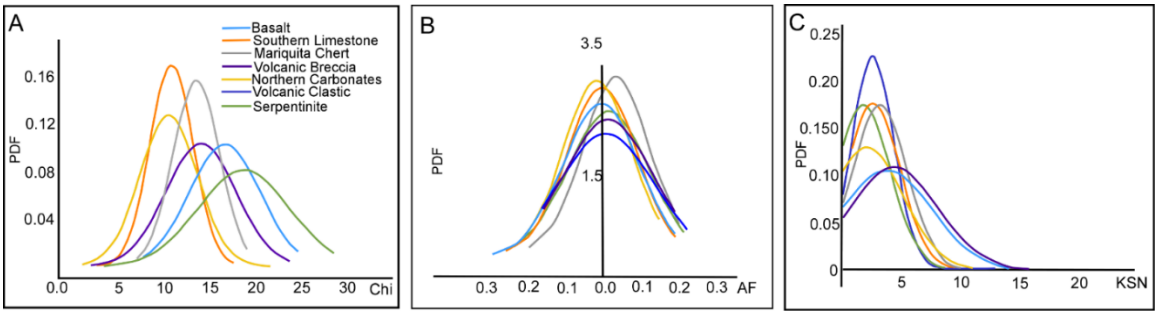

Fig. 10: Plots of the probability density function of A) Chi integral, B) Asymmetric Factor, and C) normalized steepness index (ksn) for different lithological units in Western Puerto Rico

The only lithology that displays limited correlation of the values of the PDF distribution with the lithological units is the volcaniclastic rocks for the Ksn proxy. Therefore, we argue that the results of Ksn in the volcaniclastic could be influenced by lithology, and they will not be considered further in the interpretation. In a similar way, present day precipitation patterns and climate exhibit limited correlation with the patterns of erosion and uplift observed in the χ, AF, and Ksn. Puerto Rico is divided in two distinct climatological regions. The northern two thirds of the island have a relative humid climate and the southern one third has semiarid climate (Gómez-Gómez et al., 2014). The proxies indicate high rates of erosion in Sierra Bermeja for example with a semiarid climate, and mean annual rainfall of 768 mm/yr, but they also show high rates of erosion in La Cadena de San Francisco with a humid climate and it a mean annual rain fall of 1879.6 mm/yr (Gómez-Gómez et al., 2014). Thus, our results support the hypothesis presented by previous authors of primary control of tectonic uplift over climate in the erosion of the drainage basins in active mountain ranges (e.g. Xue et al., 2018, Godard et al 2014).

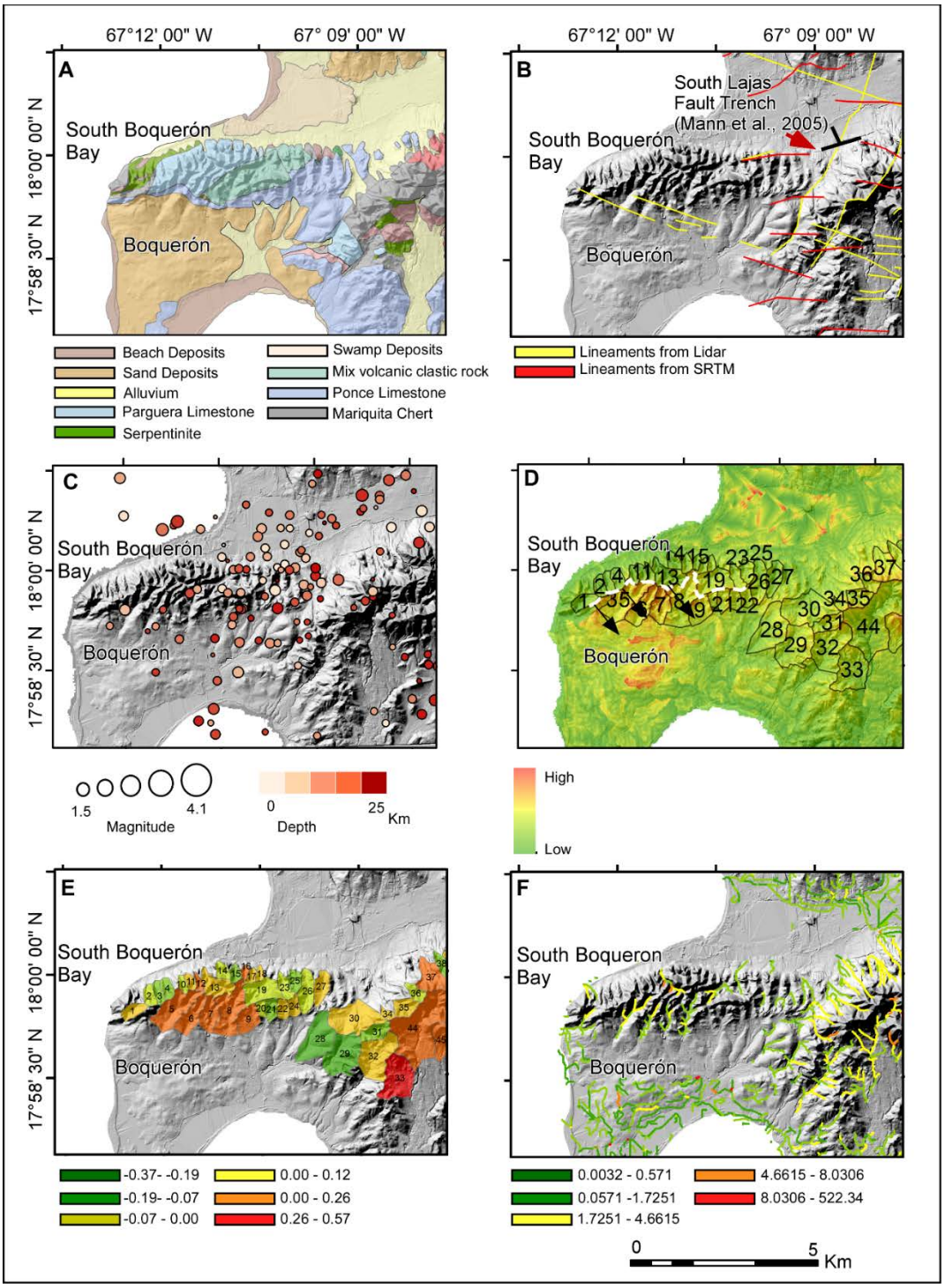

Fig 11. South Boquerón bay (Area 1 in Fig. 3) A. Geologic Map; B. Lineaments from Lidar and SRTM; C. Epicenters for earthquakes shallower than 25 km, from 1987-2017, data from Huérfano et al., 2005 and Puerto Rico Seismic Network; D. Chi integral (χ), the arrows indicate the migration direction of the drainage basins; E. Asymmetric Factor (AF), orange basins indicated highly tilted basins. F. Normalized Steepness (ksn).

It is important to mention that the three proxy's analyses was performed with data collected previous to the recent hurricane Maria, therefore, erosion patterns described in this work are not representative of that kind of catastrophic isolated events.

In addition, our results are in agreement with cosmogenic Be analysis and knick points in the Luquillo Mountains in the northeastern corner of Puerto Rico, which also support the hypothesis of dominance of tectonic uplift over the erosion patterns observed in the today's island landscape (Brocard et al., 2015). Similar results of dominance of tectonic uplift over erosion and precipitation patterns have been reported in other active tectonic landscapes like the Southeastern Ethiopian Plateau (Xue et al., 2018) and in the Himalayas (Godard et al., 2014). Understanding that tectonic uplift play primary influence in the incision rates observed in the proxies under evaluation, and climate and lithology play secondary influence in the obtained results, we will explain below the distribution pattern observed in the proxies relative to uplift.

Spatial distribution of tectonic uplift rates and drainage basin maturity

High χ values show a disequilibrium stage and tectonic uplift in the drainage divides of the mountain ranges in southern Boquerón Bay (Fig. 11 D), in Sierra Bermeja (Fig. 12D), in La Parguera (Fig. 13D), in the Punta Montalva hills (Fig. 14D) in the Sierra de Guanajibo range (Fig.15 D) and in the Cadena de San Francisco (Fig. 19D and Fig. 20D).

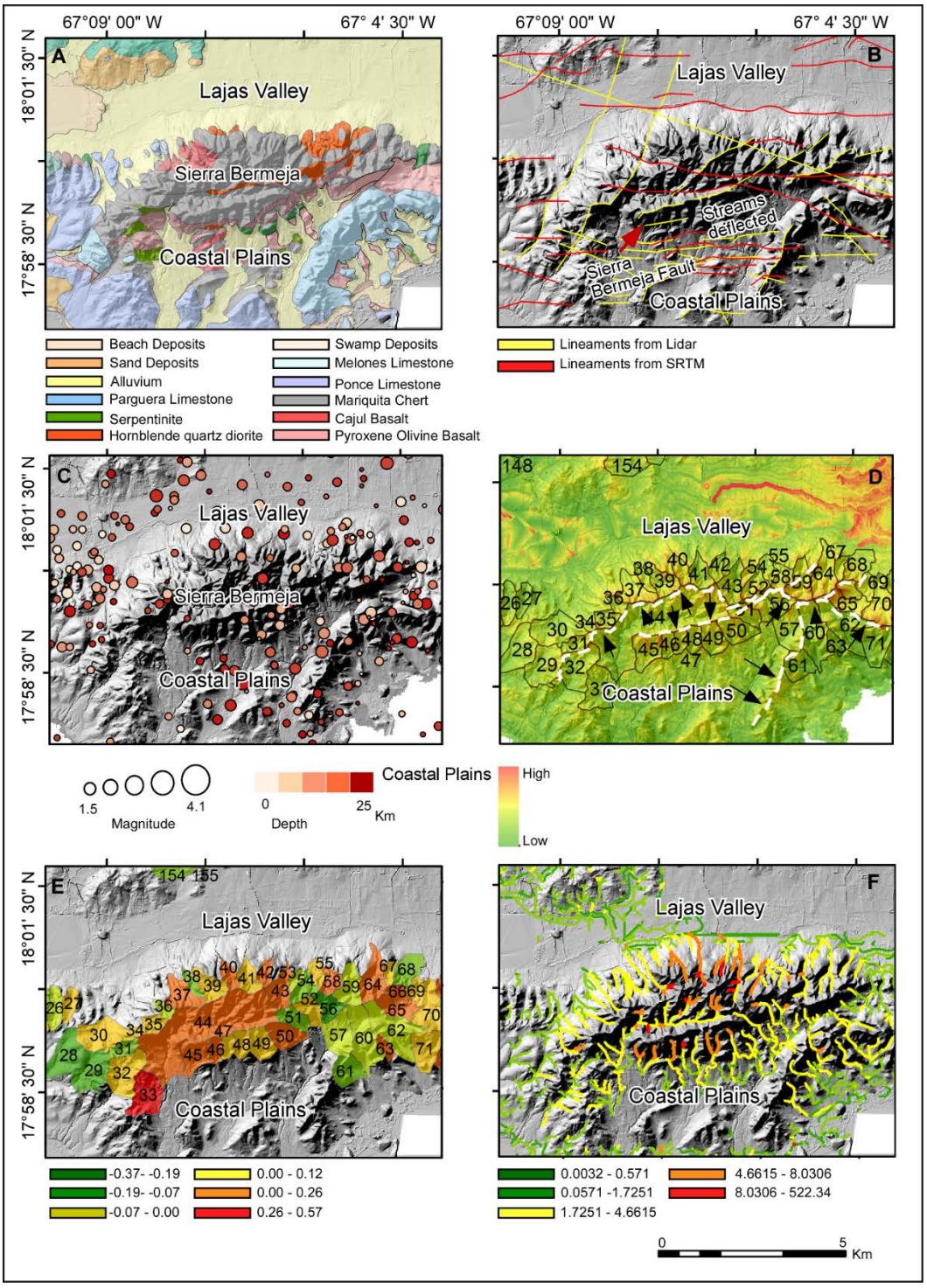

Fig 12. Sierra Bermeja (Area 2 in Fig. 3) A. Geologic Map; B. Lineaments from Lidar and SRTM; C. Epicenters for earthquakes shallower than 25 km, from 1987-2017, data from Huérfano et al., 2005 and Puerto Rico Seismic Network; D. Chi integral (χ), the arrows indicate the migration direction of the drainage basins; E. Asymmetric Factor (AF), orange basins indicated highly tilted basins. F. Normalized Steepness (ksn).

The independent proxy AF, shows highly tilted basins in southern Boquerón Bay (Fig. 11E), Sierra Bermeja (Fig. 12E), La Parguera (Fig. 13E) Punta Montalva hills (Fig. 14E), Guánica (Fig. 15E) and in Cerro Goden Fault (Fig 19E and 20E). These are the same areas where χ is showing sharp change along the drainage divides. Nevertheless, AF does not show correlation in the Sierra de Guanajibo mountain range (Fig 17E). These could be happening because the drainage basins are not tilted enough to be captured by the AF proxy.

The normalized steepness (Ksn) index also shows different rates of erosion along the river profiles consistent with the areas in disequilibrium showed by the χ and AF in South Boquerón Bay (Fig. 11F), Sierra Bermeja (Fig. 12F), La Parguera (Fig. 13F), Punta Montalva (Fig. 14F), Guánica (Fig. 15F), in the Sierra de Guanajibo (Fig. 17F) and Cerro Goden Fault (Fig. 19F and Fig 20F).

The high values of the χ, AF, and ksn indicating disequilibrium and tectonic uplift on the basins are also consistent with the distribution of earthquakes and lineaments observed from Lidar DEMs and SRTM DEMs in south Boquerón Bay (Fig 11B and 11C), Sierra Bermeja (Fig. 12B and 12C), La Parguera (Fig. 13B and 13C), the Sierra de Guanajibo range (Fig. 17B and 17C), and La Cadena de San Francisco Range (Fig. 19B, 19C, 20B and 20C). With this additional piece of evidence, we argue that the disequilibrium observed in the drainage basins could be related to local uplift and therefore to active faulting. Moreover, uplift activity in the mentioned areas has been suggested by previous studies.

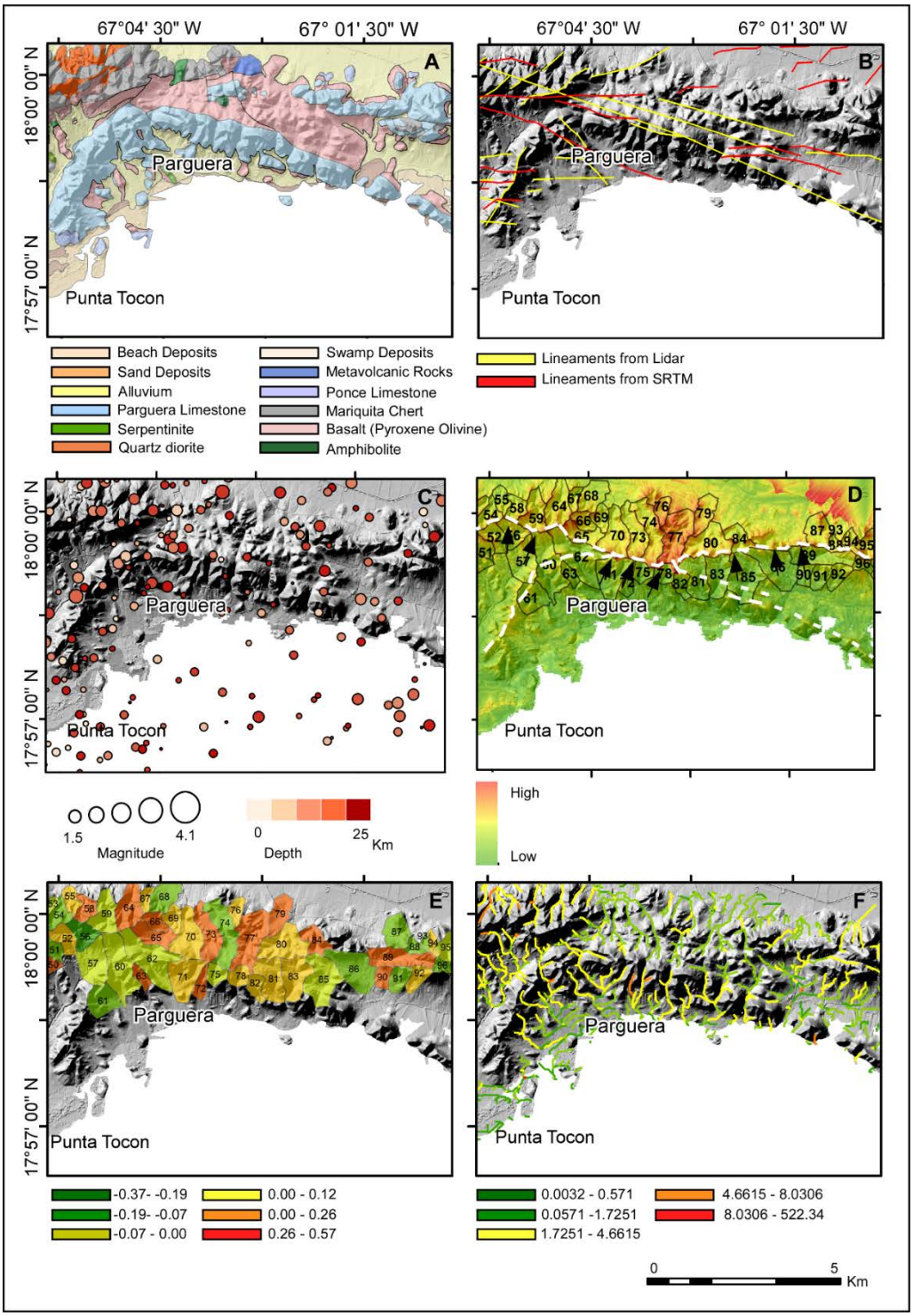

Fig 13. La Parguera (Area 3 in Fig. 3) A. Geologic Map; B. Lineaments from Lidar and SRTM; C. Epicenters for earthquakes shallower than 25 km, from 1987-2017, data from Huérfano et al., 2005 and Puerto Rico Seismic Network; D. Chi integral (χ), the arrows indicate the migration direction of the drainage basins; E. Asymmetric Factor (AF), orange basins indicated highly tilted basins. F. Normalized Steepness (ksn).

Area 1: South Boquerón Bay

In south Boquerón Bay, the proxies show tectonic uplift (Fig.11). In addition, published geologic maps show a possible E-W striking fault cutting the Oligo-Miocene units (Mattson, 1960; Briggs and Akers, 1965).

According to Mattson (1960), the fault is concealed to the east where is covered by the alluvium and truncated by another N-NW striking fault. Briggs and Akers (1965) suggest that it continues further to the east until the base of Sierra Bermeja. Faults in this area where inferred to have left lateral strike slip movement with a normal component because the relative movement between the Caribbean and North American Plate (Almy, 1969; Volckman 1984b). The uplift signals observed in the proxies in South Boquerón bay indicate a recent normal component in the fault. In addition, the signals indicate a possible trace that extend to the west of the trace described by Briggs and Akers (1965) and bordering the serpentine unit (Fig. 11D, Fig. 11E and Fig. 11F). The signal disappears a few km from the coast to the west and to the east its covered by the alluvium (Fig.11D, Fig. 11E and Fig. 11F).

In the previously reported South Lajas fault by trenching studies the proxies in this area do not display a clear signal, this could be because the uplift is too low to be recorded at the resolution of the data.

Area 2: Sierra Bermeja

The proxies show tectonic uplift in the southern and northern branch of the Sierra Bermeja range (Fig. 12). A vertical fault was described in the southern branch of the Sierra Bermeja range (Mattson, 1960; Briggs and Akers, 1965) in the same location

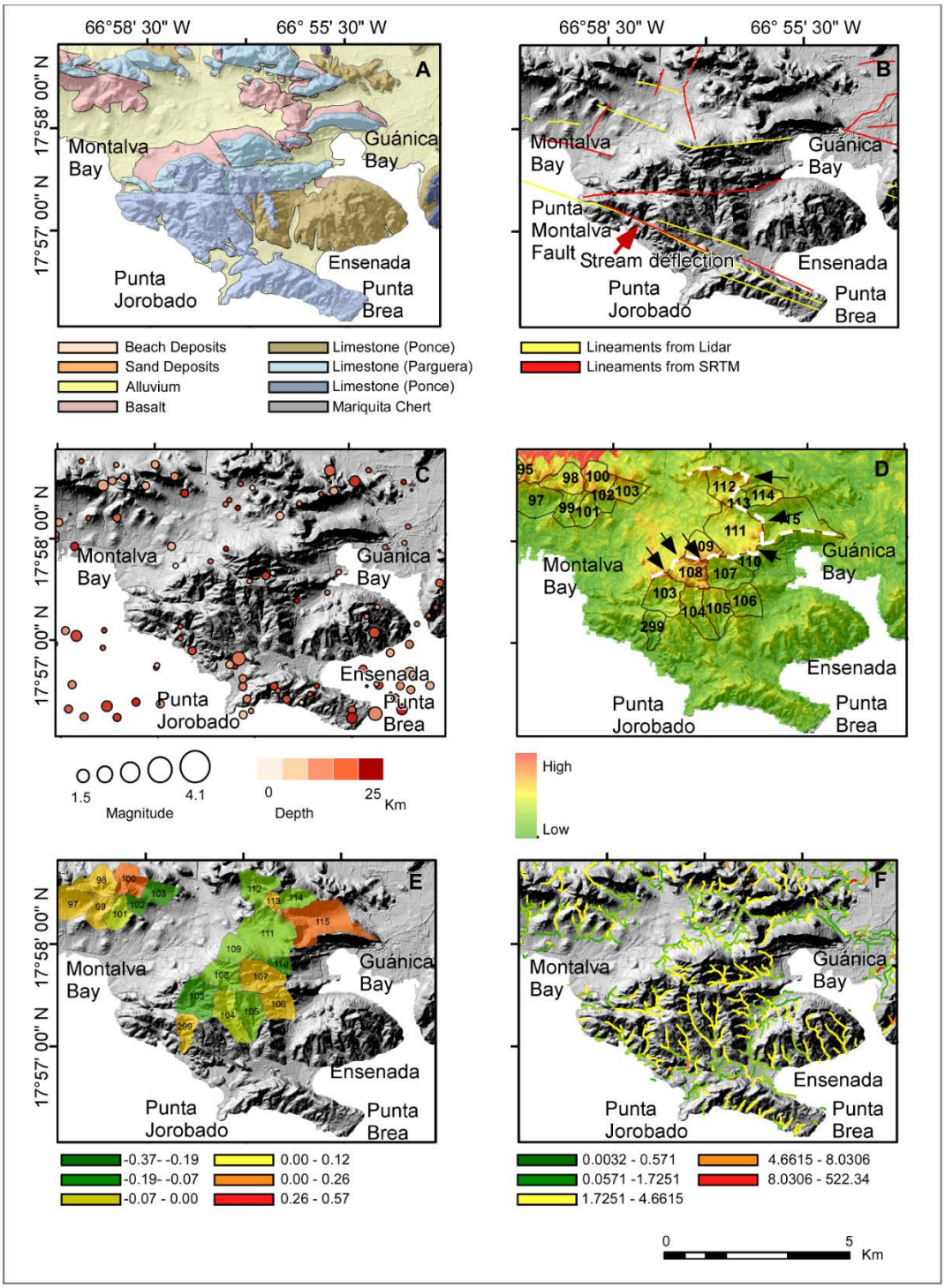

Fig 14. Punta Montalva (Area 4 in Fig. 3) A. Geologic Map; B. Lineaments from Lidar and SRTM; C. Epicenters for earthquakes shallower than 25 km, from 1987-2017, data from Huérfano et al., 2005 and Puerto Rico Seismic Network; D. Chi integral (χ), the arrows indicate the migration direction of the drainage basins; E. Asymmetric Factor (AF), orange basins indicated highly tilted basins. F. Normalized Steepness (ksn)

where the uplift, tilted drainage basin and high difference of rate of erosion is observed in the proxies (Fig 12D, Fig. 12E and Fig. 12F). In the northwestern edge of Sierra Bermeja, a high angle fault was mapped and interpreted as subparallel to South Lajas fault zone (Volckman 1984a; Mann et al., 2005). In this area, the signal of the pattern of migration does not follow a linear trend. Instead, it seems to be moving from the center of the range outward suggesting that the area is accommodating strain from tectonic uplift. The faults in this area affecting the basement rock of Sierra Bermeja was interpreted to have northeast orientation as the signal observed in the proxies and to have preferential Holocene reactivation (Mann et al., 2005).

Area 3: La Parguera

In La Parguera, a geomorphic signal of disequilibrium and uplift activity is observed in the northern side of the Parguera hills (Fig 13D, 13E and 13F). The proxies show the drainage basins disequilibrium contradicting the recent studies (Mann et al., 2005) and supporting the hypothesis of faulting by Mattson (1960), showing a small area of strong signal of active faulting (Fig. 13D).

Area 4: Punta Montalva

In Punta Montalva, the proxies show a small area of uplift cutting the Ponce Limestone in northeast direction (Fig 14D, 14E and 14F). The uplift is located northwest to the previously reported Punta Montalva fault which is clearly identifiable in our Lidar DEM by river deflection (Fig. 14B). Nevertheless, the Punta Montalva fault does not show a clear signal in the proxies because the fault does not have a normal component.

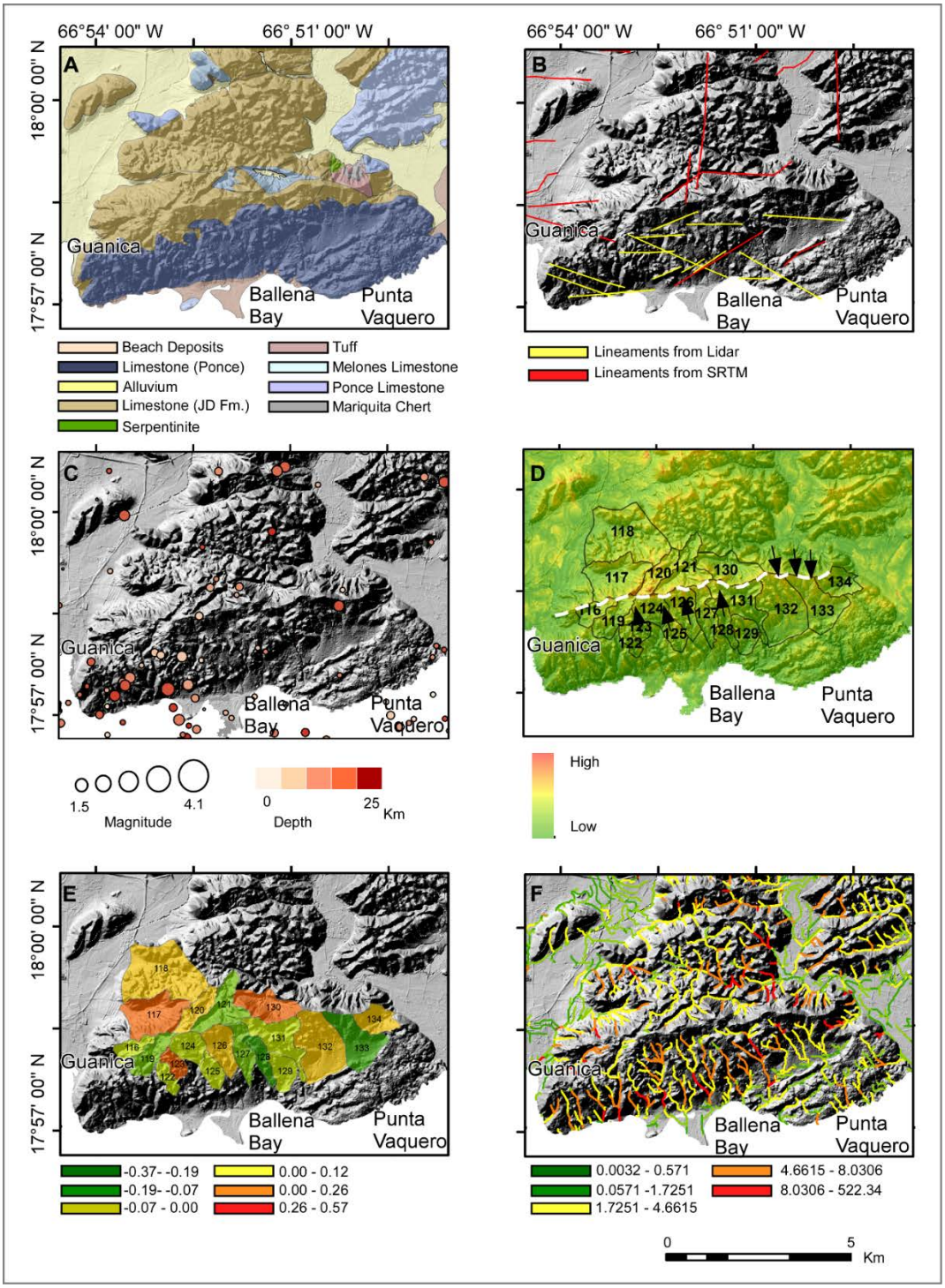

Fig 15. Guánica (Area 5 in Fig. 3) A. Geologic Map; B. Lineaments from Lidar and SRTM; C. Epicenters for earthquakes shallower than 25 km, from 1987-2017, data from Huérfano et al., 2005 and Puerto Rico Seismic Network; D. Chi integral (χ), the arrows indicate the migration direction of the drainage basins; E. Asymmetric Factor (AF), orange basins indicated highly tilted basins. F. Normalized Steepness (ksn).

Previous studies connect the fault in Punta Montalva with Parguera and North Boquerón bay in long fault system cutting obliquely the Lajas valley (Mattson, 1960; Roig-Silva et al., 2013). The uplift area identified northwest from the Punta Montalva fault is unmapped by previous research.

Reported focal mechanism solution of local events in Punta Montalva suggest a component of compression which will justify the signal of local uplift and high change of rate of erosion evidence by the proxies and a component of left-lateral strike slip which account for Punta Montalva Fault (Roig-Silva 2013).

Area 5: Guánica

In Guánica, the χ show a weak signal of uplift cutting the Ponce limestone units to the northeast (Fig. 15D). However, ksn show high variation in the rates of erosion following a similar trend than the weak signal observed in χ (Fig. 15D and Fig. 15 F). Guánica belongs to the south dipping Oligocene-Pliocene sedimentary carbonate rocks on the southern edge of Puerto Rico arch (Mann et al., 2005). In addition to the uplift signal observed in the proxies, stream deflection was found in the Lidar DEMs in the western corner of the carbonate platform located in the coast. The sense of motion observed in the stream deflection is left-lateral and match the occurrence of earthquakes in the area (Fig. 15B and 15C). Focal mechanism solutions in Guánica also suggest strike-slip motion (Huérfano et al., 2005). Previous recent research has not reported active faulting in Guánica area, however, the limestone of Juana Diaz Formation may be uplifted against the Ponce Limestone (Monroe 1973).

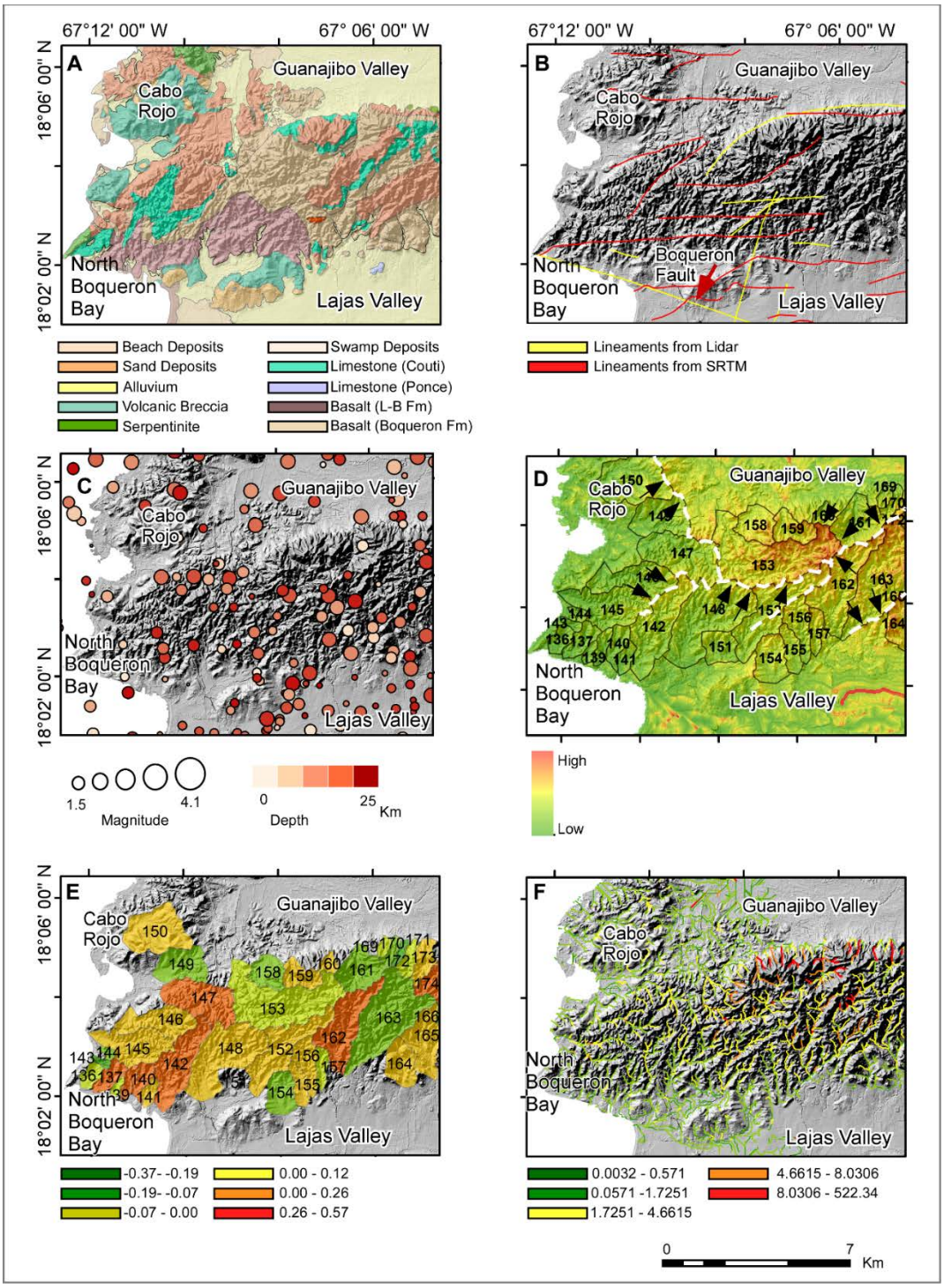

Fig 16. Northern Boquerón Bay (Area 6 in Fig. 3). A. Geologic Map; B. Lineaments from Lidar and SRTM; C. Epicenters for earthquakes shallower than 25 km, from 1987-2017, data from Huérfano et al., 2005 and Puerto Rico Seismic Network; D. Chi integral (χ), the arrows indicate the migration direction of the drainage basins; E. Asymmetric Factor (AF), orange basins indicated highly tilted basins. F. Normalized Steepness (ksn).

Area 6: North Boquerón Bay

In North Boquerón Bay, the proxies do not record uplift, or significant differential erosion (Fig.16D, 16E and 16F). This suggests that the North Boquerón Bay fault does not have a dip-slip component.

Area 7: Sierra de Guanajibo

In the Sierra de Guanajibo mountain range, in San Germán quadrangle, a strong signal of uplifting is observed in the proxies delineating the Eocene thrusting San Germán Fault (Fig. 17D, 17E, 17F). In addition, another strong signal south of the San Germán Fault delineate another thrust fault. This fault was also characterized by previous researchers as the Yauco Formation thrusting over El Rayo Formation (Volckmann 1984b, Laó-Dávila et al., 2012). Relative dating of the thrust faults were suggested to be before late Eocene because a dike cuts the serpentine belts. Disequilibrium of the drainage basins suggesting uplift observed in the proxies indicate a more recent reactivation of the faults with at least a normal component in San Germán area.

Area 8: Northeastern Lajas

In northeastern Lajas and Sabana Grande, a strong signal of uplifting was observed in the proxies delineating the previously reported Eocene Torre Fault (Fig. 18 D, Fig. 18E, Fig. 18F; Slodowski et al. 1956). However, the disequilibrium of the drainage basins indicating uplift, observed in the proxies suggests recent reactivation of the Torre Fault. Due to the high seismicity in the Lajas valley, reactivation of older faults is a plausible hypothesis.

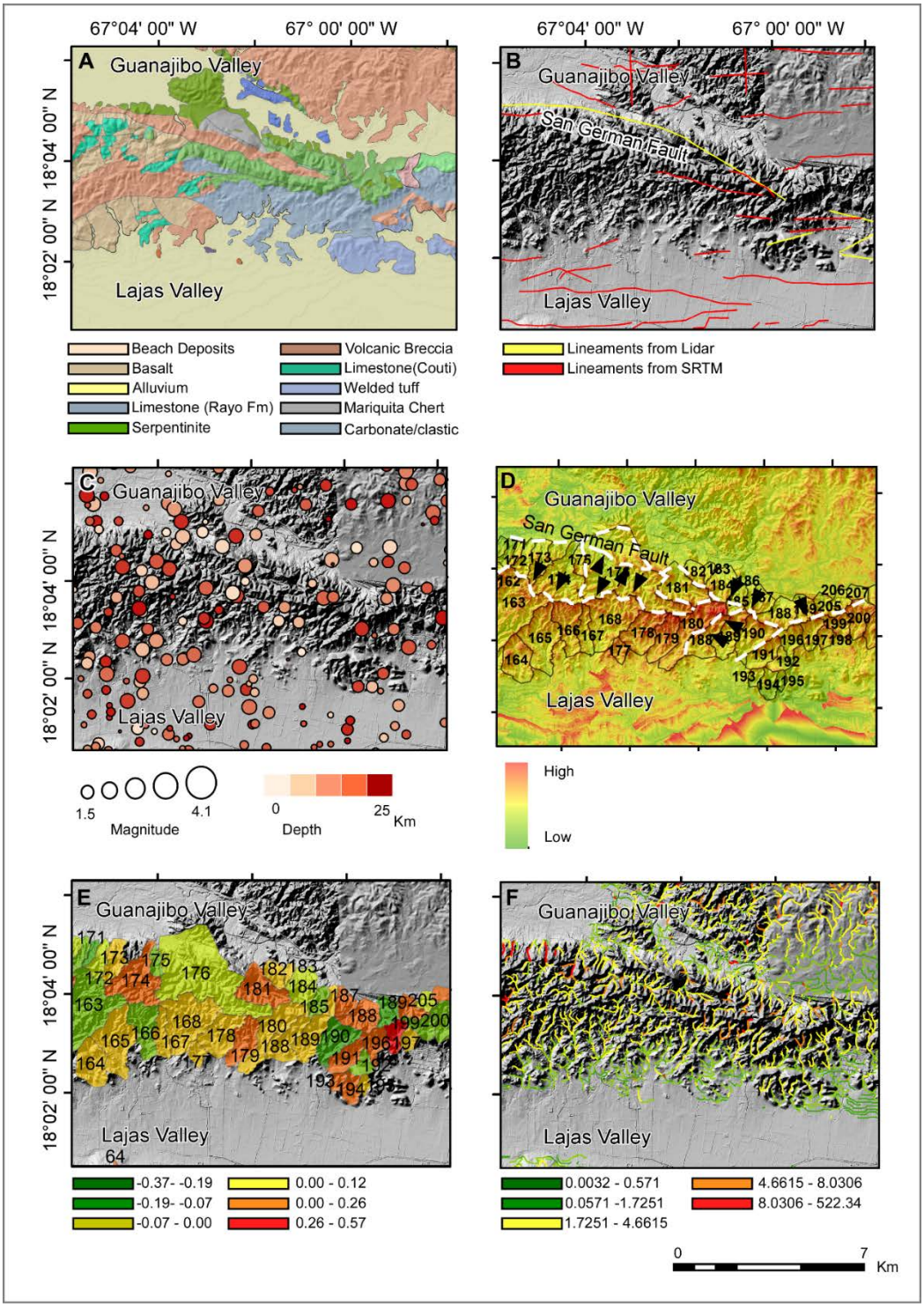

Fig 17. The Sierra de Guanajibo (Area 7 in Fig. 3). A. Geologic Map; B. Lineaments from Lidar and SRTM; C. Epicenters for earthquakes shallower than 25 km, from 1987-2017, data from Huérfano et al., 2005 and Puerto Rico Seismic Network; D. Chi integral (χ), the arrows indicate the migration direction of the drainage basins; E. Asymmetric Factor (AF), orange basins indicated highly tilted basins. F. Normalized Steepness (ksn).

Recent focal mechanism solutions are consistent with the NW-SE direction with a normal component and support the hypothesis of active faulting (Huérfano et al., 2005).

Areas 9 and 10: Cerro Goden Fault

In La Cadena de San Francisco, we found a signal of uplift and high erosion recorded by the proxies (Fig. 19 and Fig. 20). However, the χ proxy's signal trace is located in the crest of La Cadena de San Francisco, north of the Cerro Goden Fault (Fig. 19D and Fig. 20D; Mann et al., 2005). No strong signal is recorded to the west of the range and close to the coast with χ and AF proxies (Fig. 19D and Fig. 19E), suggesting that the basins located along in the Añasco bay are close to equilibrium state. Nevertheless, the Ksn proxy report high variation of rate of erosion along the southern flank of La Cadena de San Francisco from west to east (Fig. 19 F anf Fig. 20F) and AF shows highly tilted basins to the west (Fig. 19E and Fig. 20F). Our results correlate the previous research observation about more evidence of movement to the east than to the west.

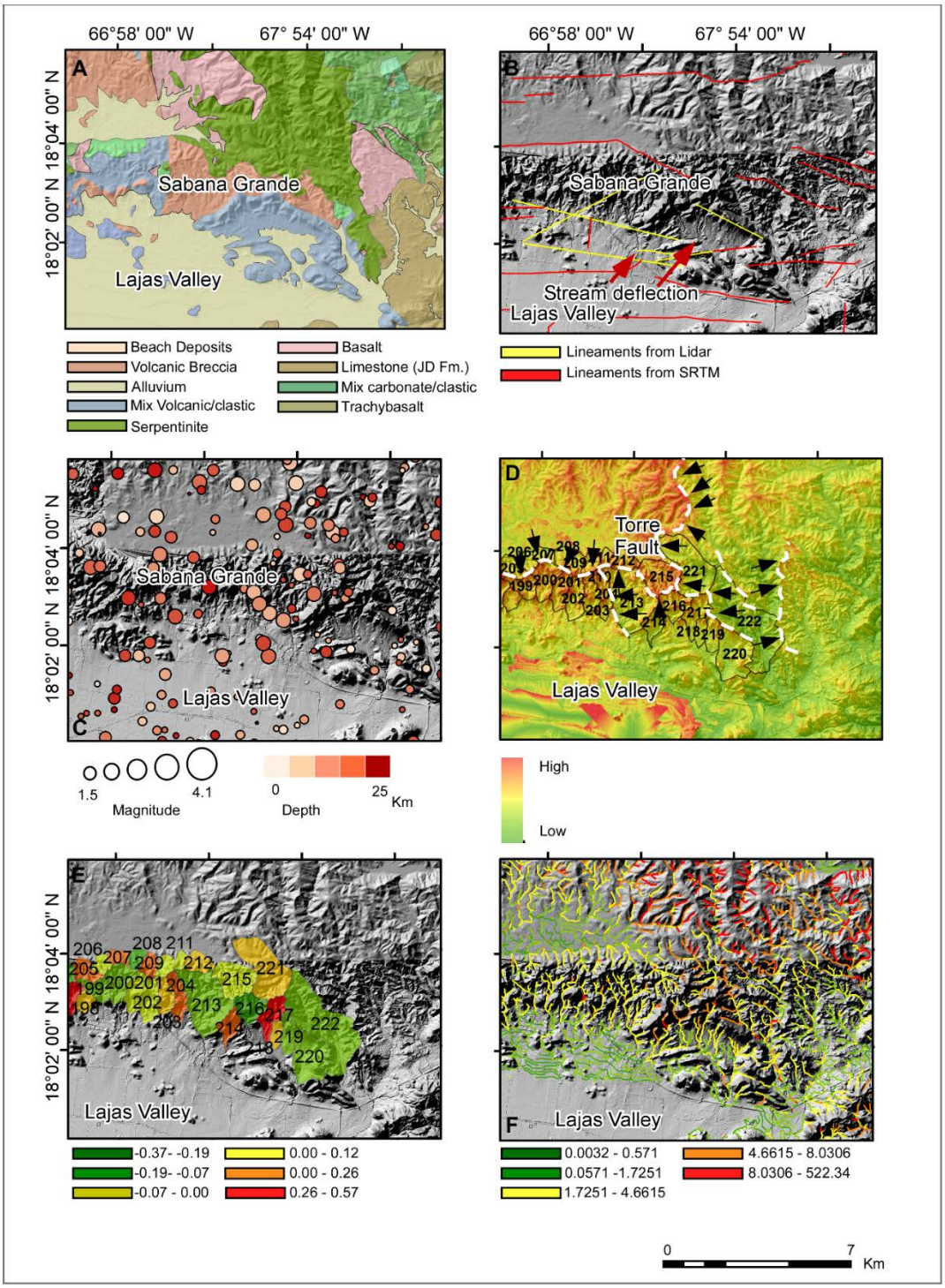

Fig 18. Northeastern Lajas (Area 8 in Fig. 3). A. Geologic Map; B. Lineaments from Lidar and SRTM; C. Epicenters for earthquakes shallower than 25 km, from 1987-2017, data from Huérfano et al., 2005 and Puerto Rico Seismic Network; D. Chi integral (χ), the arrows indicate the migration direction of the drainage basins; E. Asymmetric Factor (AF), orange basins indicated highly tilted basins. F. Normalized Steepness (ksn).

Active tectonics implication for western Puerto Rico and plate margin.

Proxies show strong signal of uplift related to tectonics in Cerro Goden Fault and south Lajas Valley, areas previously suggested by several studies to be affected by active faulting. Signal of uplift is higher in both sites and stronger to the east, indicating along strike variation from east to west, and possible relation of uplift with South Puerto Rico Fault Zone (Fig. 1B). Uplift in Lajas Valley have been also suggested by trenching studies in the Holocene South Lajas Fault (Prentice and Mann, 2005); fault striation from Miocene rocks (Hippolyte et al., 1995 and Mann et al., 2005), and geophysical surveys offshore western Lajas Valley (Grindlay et al., 2005). Uplift was also suggested by recent studies in eastern Lajas Valley in the Holocene Salinas Fault, south of South Puerto Rico Fault Zone. In addition, southwestern Puerto Rico have been recognized to be the focus of active seismicity occurring in the island (Huérfano et al., 2005).

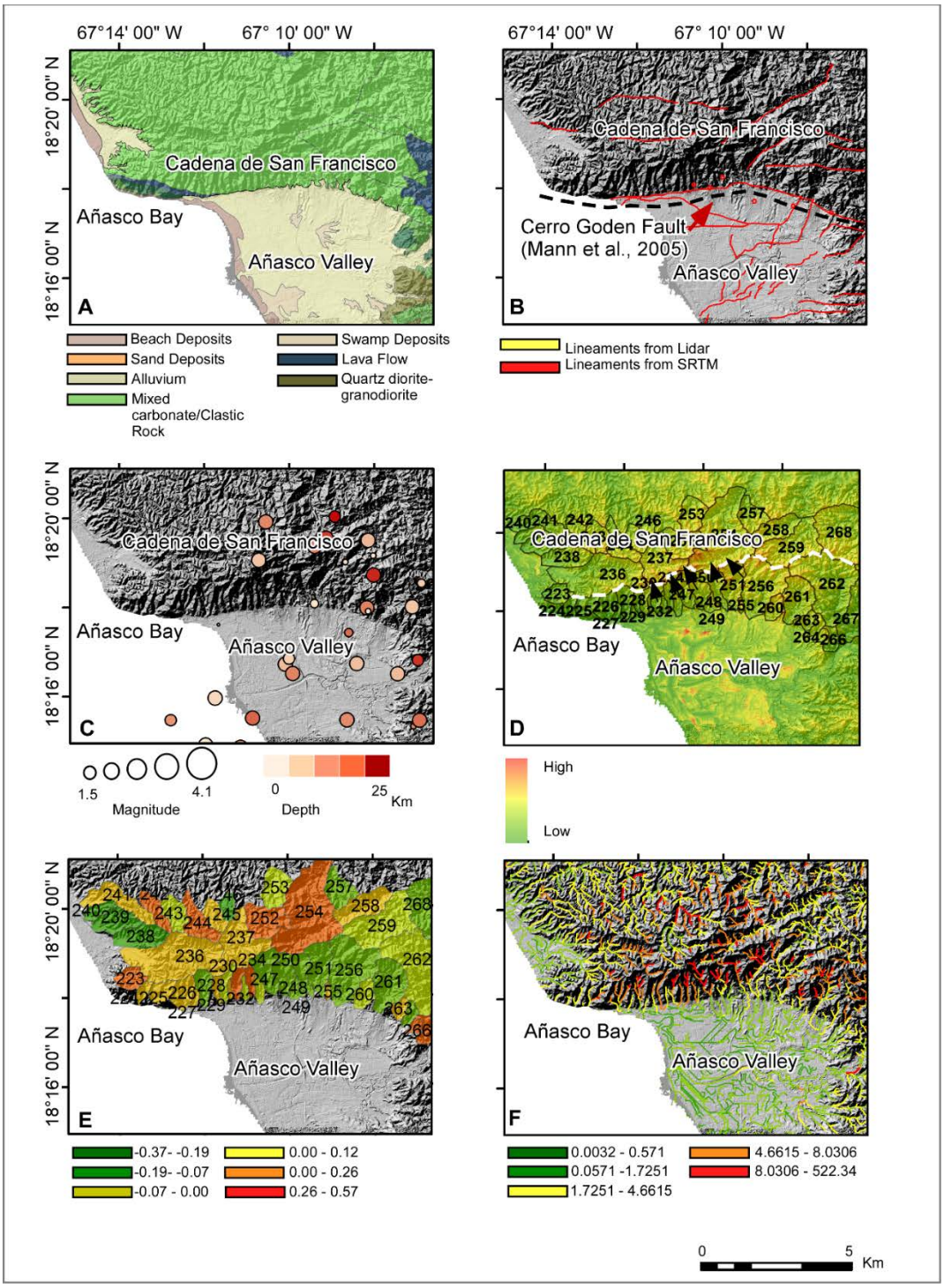

Fig 19. Western Goden Fault (Area 9 in Fig. 3). A. Geologic Map; B. Lineaments from Lidar and SRTM; C. Epicenters for earthquakes shallower than 25 km, from 1987-2017, data from Huérfano et al., 2005 and Puerto Rico Seismic Network; D. Chi integral (χ), the arrows indicate the migration direction of the drainage basins; E. Asymmetric Factor (AF), orange basins indicated highly tilted basins. F. Normalized Steepness (ksn).

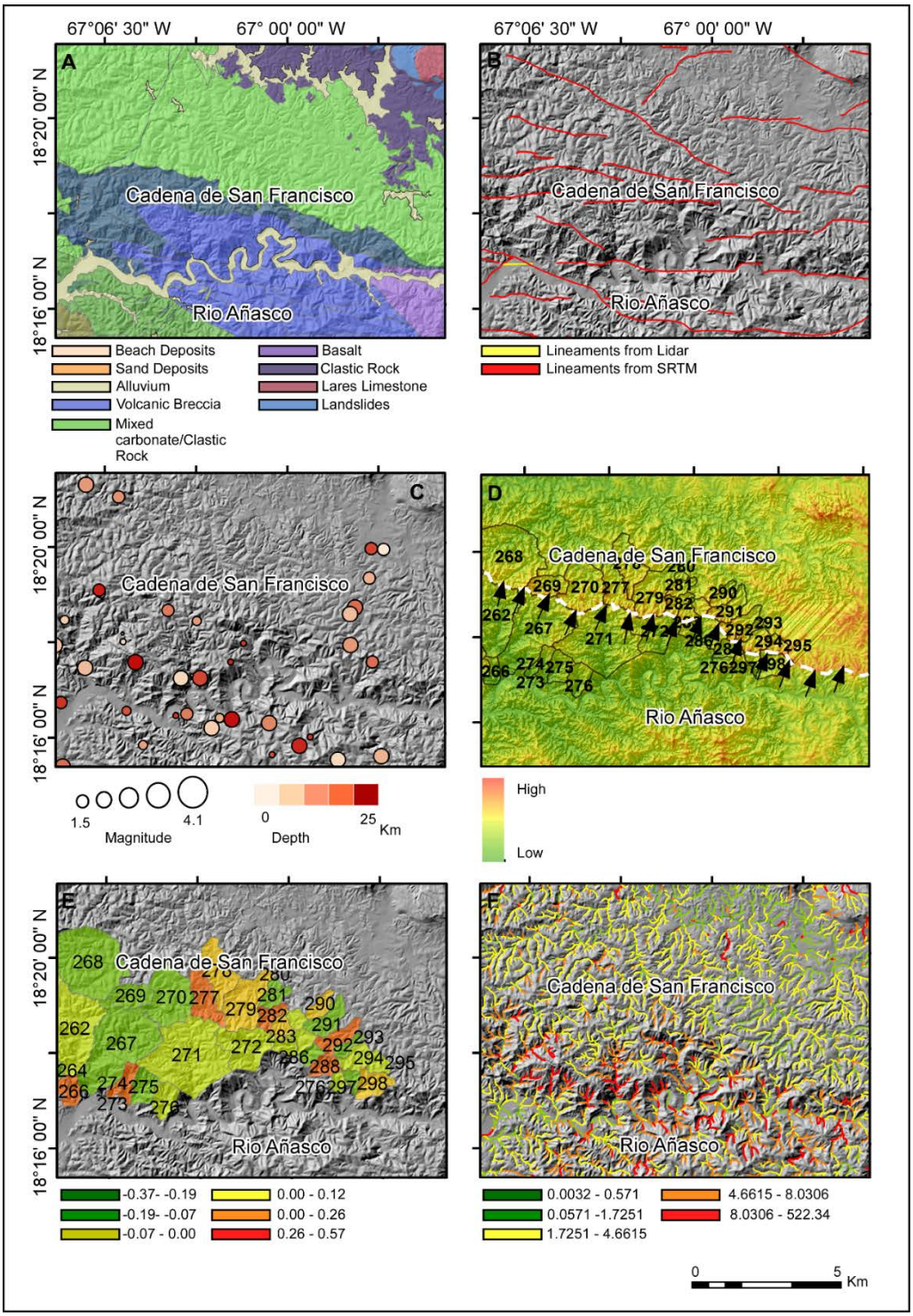

Fig 20. Eastern Goden Fault (Area 10 in Fig. 3). A. Geologic Map; B. Lineaments from Lidar and SRTM; C. Epicenters for earthquakes shallower than 25 km, from 1987-2017, data from Huérfano et al., 2005 and Puerto Rico Seismic Network; D. Chi integral (χ), the arrows indicate the migration direction of the drainage basins; E. Asymmetric Factor (AF), orange basins indicated highly tilted basins. F. Normalized Steepness (ksn).

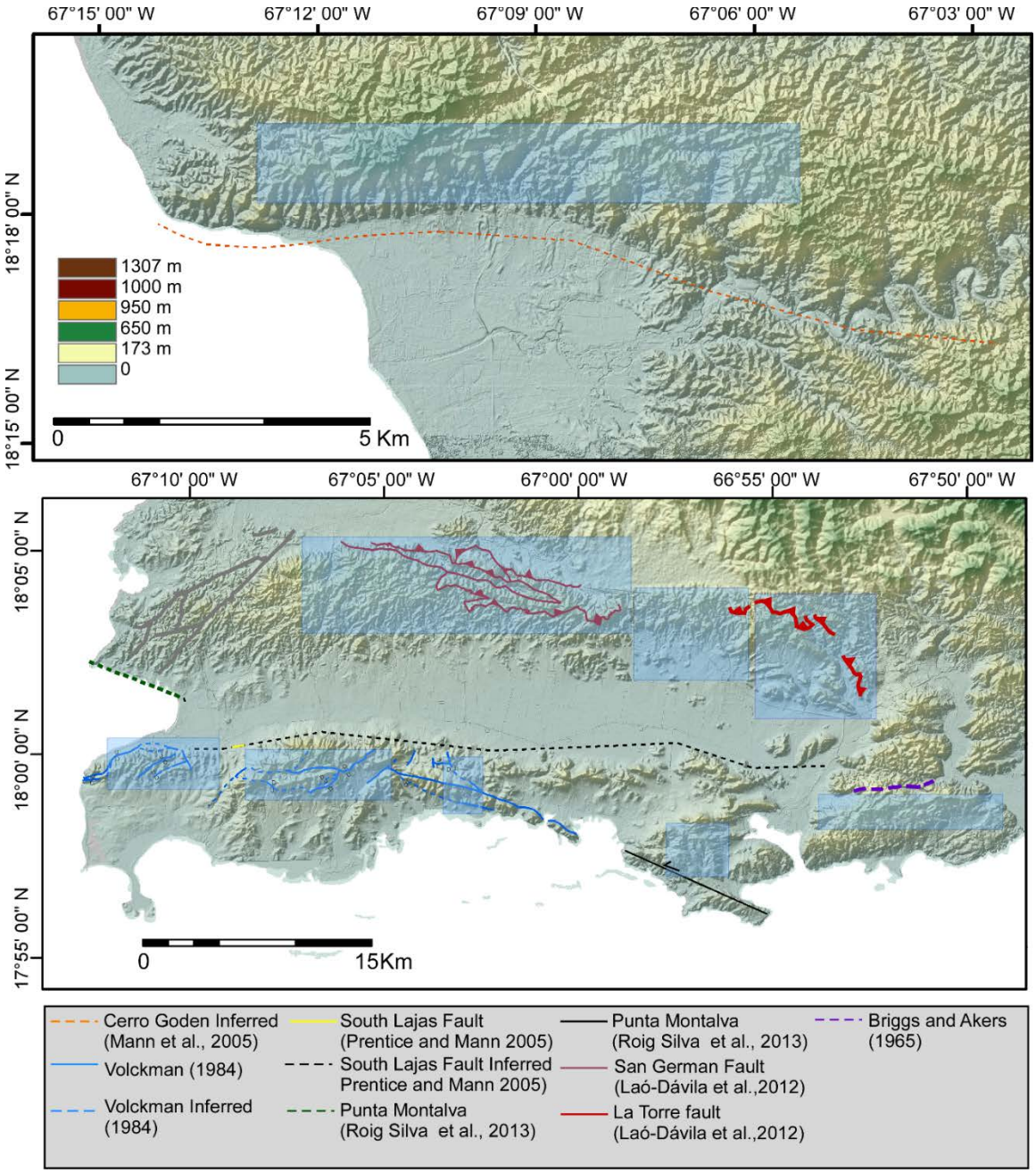

Fig 21. Faults suggested by previous researchers. Transparent boxes indicate areas where the proxies indicate uplift.

CHAPTER VI

CONCLUSION

After combining the analysis of three geomorphic proxies χ, AF, and ksn with lithology, microseismicity, active faulting, and data of previous research, we were able to provide spatial and patterns suggestive of tectonic uplift rate in western Puerto Rico. We found that (i) Geomorphic proxies show significant results in subduction zones with very low tectonic uplift and they also provide important insights on final detailed geology (ii) The spatial distribution of geomorphic proxies values suggests more uplift and tectonic activity to the northeast of Lajas Valley than in the south, whereas in Cerro Goden Fault the east seems more active to the west (iii) Proxies suggest tectonic uplift in South Boquerón Bay close to the coast which could be related to Lajas Valley fault, also signal of uplift is suggested in La Parguera and Guánica (iv) Geomorphic proxies suggest possible reactivation of older structures like Sierra Bermeja fault, San Germán and Torre fault.

We provided not only provided meaningful results regarding to the use of geomorphic proxies in subduction zones with very low uplift rate but also provided further evidence of tectonic forces exerting primary influence in the geomorphic pattern prevalent today in western Puerto Rico. Furthermore, we provided important insights in areas of active faulting suggested by previous authors like Cerro Goden Fault (Mann et

al., 2005), in new areas of south Boquerón Bay, La Parguera, Punta Montalva and Guánica. In addition, we were able to indicate possible reactivation of faults in Sierra Bermeja and in the northeastern side of the Lajas Valley, San Germán and la Torre fault.

Future work recommendations

1) Process geomorphic proxies with 1m resolution with the soon to be released LiDAR Data.

2) Perform paleoseismic studies in the Areas where geomorphic proxies have shown higher signal of uplift: northeaster Lajas Valley and eastern Cerro Goden Fault.

3) Process geomorphic proxies in North Puerto Rico Fault Zone and in South Puerto Rico Fault Zone.

4) Process geomorphic proxies in southeastern Puerto Rico where some recent seismicity have been reported

REFERENCES

Almy C., Jr., 1969, Sedimentation and tectonism in the Upper Cretaceous Puerto Rican portion of the Caribbean island arc: Transactions of the Gulf Coast Association of Geological Science, v.19, p. 269-279.

Arrowsmith, R., and Zielke O., 2009, Tectonic geomorphology of the San Andreas Fault zone from high-resolution topography: An example from Cholame segment: Geomorphology, no. 113, p. 70-81.

Ascencio, E., 1980. Western Puerto Rico Seismicity: U. S. Geological Survey Open-File Report p. 80-192, 135.

Brocard, G., Y., Willenbring J., K., Miller T., E., Frederik S., N., Johnson A., H., 2015, Effects of a tectonically-triggered wave of incision on riverine exports and soil mineralogy in the Luquillo Mountains of Puerto Rico : Applied Geochemestry, no. 63, p. 586-598.

Briggs, R., P., and Akers, J., P., 1965, Hydrogeologic map of Puerto Rico and adjacent islands: U.S. Geological survey Hydrological Investigations Atlas HA-197, scale 1:240,000.

Burke, K., Cooper, C., Dewey, J. F., Mann, J. P., Pindell, J., 1984, Caribbean tectonics and relative plate motions: The Caribbean South American Plate Boundary and Regional Tectonics. Geol. Soc. Am. Mem. 162. 421 pp.

Byrne, D. B., Suarez, G., and McCann W.R., 1985, Muertos Trough subduction-Microplate tectonics in the northern Caribean: Nature, v. 317, p. 420-421.

Calais, E., Symithe, S., Mercier., B., Prépetit C., 2015 Plate boundary segmentation in the northeastern Caribbean from geodetic measurements and Neogene geological observations: C.R. Geoscience, no. 348, p. 42-51.

Chen, Y.C., Sung Q.C., Cheng., K., 2003, Along-strike variations of morphotectonic features in the Western Foothills of Taiwan: tectonic implication based on stream gradient and hypsometric analysis: Geomorphology 56 (1-2), 109-137.

Cowie, P., A., Attal, M., Tucker, G., E., Whittaker, A., C., Naylor, M., Ganas, A., Roberts G., P., 2006, Investigating the surface process responses to fault interaction and linkage using a numerical modelling approach: Basin Research, no.18, p. 231-266.

DeMets, C., Jansma P., Mattiolli G., Dixon, T., Farina, F., Bilham, R., Calais E. and Mann, P., 2000, GPS geodetic constraind on Caribbean-North America plate motion: Geophysical Research Letters, no. 27, p. 437-440.

Donellan, A., Arrowsmith, R., Langenheim, V., 2015, Select Airborne Techniques for Mapping and Problem Solving, in Applied Geology in California eds. R. Anderson and H. Ferriz, Star Publishing, California, p. 541-566.

Dominguez-González, L., Andreani, L., Stanek, K., P., Gloaguen, R., Geomorphotectonic evolution of the Jamaican restraining bend: Geomorphology no. 228, p. 320-334.

Ferraris, F., Firpo M., Pazzaglia F., 2012, DEM analyses and morphotectonic interpretation: The Plio-Quaternary evolution of the eastern Ligurian Alps Italy: Geomorphology, no. 149-150, p. 27-40.

Grindlay, N.R., Abrams, L.J., Del Greco L., and Mann, P., 2005, Toward an integrated understanding of Holocene fault activity in western Puerto Rico: Constraints from high resolution seismic and sidescan sonar data, in Mann, P., ed., Active Tectonics and seismic hazards of Puerto Rico, Virgen Island, and offshore areas: Geological Society of America Special Papers 385, p. 139-160.

Glover III, L., 1971. Geology of Coamo area, Puerto Rico and its relation to the volcanic arc-trench association: U.S. Geological Survey. Prof Pap 636,102.

Gómez-Gómez, F., Rodríguez-Martínez, J., Santiago, M., Hydrogeology of Puerto Rico and the outlying islands of Vieques, Culebra and Mona: U.S. Geological Sur0vey Scientific Investigations Map 3296, 40 p. plus 2 pls., http://dx.doi.org/10.3133/sim3296.

Godard, V., Bourlès, D., L., Spinabella, F., Burbank, D., W., Bookhagen, B., Fisher, G., B., Moulin, A., Léanni, L., 2014 Dominance of tectonics over climate in Himalayan denudation: Geology, no. 3. p. 243-246

Hippolyte, J. C., Mann, P., Grindlay, N., 2005, Geologic evidence for the prolongation of active normal faults of the Mona Rift into northwestern Puerto Rico, in Mann, P., ed., Active Tectonics and seismic hazards of Puerto Rico, Virgen Island, and offshore areas: Geological Society of America Special Papers, no. 385, p. 161-171.

Howard, A., D., Dietrich, W., E., Seidl, M., A., 1994, Modeling fluvial erosion on regional to continental scale: Journal of Geophysical Research of Solid Earth, no. 99, p. 13971-13986.

Hudnut, K. W., A. Borsa, C. Glennie, and J.-B. Minster, 2002 High-resolution topography along surface rupture of the 16 October 1999 Hector Mine, California, earthquake

(Mw7.1) from airborne laser swath mapping, Bulletin of Seismolical Society of America v. 92, no. 4, 1570-1576.

Huérfano, V., von Hillebrandt-Andrade, C., and Báez Sánchez, G., 2005, Microseismicity activity reveals two stress regimes in southwestern Puerto Rico, in Mann, P., ed., Active Tectonics and seismic hazards of Puerto Rico, Virgen Island, and offshore areas: Geological Society of America Special Papers, no. 385, p. 81-101.

Ismail, E., H., Abdelsalam, M., G., 2014, Morpho-tecttonic analysis of the Tekeze River and the Blue Nile drainage system on the Northwestern Plateau, Ethiopia: Journal of African Earth Science, no 69, p. 34-47.

Isemburg, M., 2016, LASzip: lossless compression of LiDAR data: [Online], http://laszip.org

Jansma, P. E., Mattioli, G. S, Lopez, A., DeMetts, C., Dixon, T., Mann, P., Calais, E., 2000, Neotectonics of Puerto Rico and the Virgen Island, northeastern Caribbean, from GPS geodesy: Tectonics, no. 19, p. 1021-1037.

Jansma, P. E., Mattioli, G. S., 2005, GPS results from Puerto Rico and the Virgen island: constrains on tectonics setting and rates of active faulting, in Mann, P., ed., Active Tectonics and seismic hazards of Puerto Rico, Virgen Island, and offshore areas: Geological Society of America Special Papers 385, p. 13-30.

Jolly, W. T., Lidiak E. G., Schellekens, J. H., and Santos, H., 1998. Volcanism, tectonics, and stratigraphic correlations in Puerto Rico: Tectonics and geochemistry of the Northeastern Caribbean, in Lidiak, E.G., and Laure, D.K., eds., Tectonic and Geochemestry of Northeastern Caribbean: Geological Society of American Special Paper 322, p. 1-34.

Kirby, E., Whipple, K.X., Tang., W., Chen Z.L., 2003. Distribution of active uplift along the eastern margin of the Tibetean Plateu: inferences from bedrock channel longitudinal profiles. Journal of Structural Geology 44, p. 54-75.

Laó-Dávila, D. A., and Anderson, T., H., 2009, Kinematic analysis of serpentinite and manifestation of transpression in southwestern Puerto Rico: Journal of Structural Geology, 31, p. 1472-1489, doi:10.1016/j.jsg.2009.09.008.

Laó-Dávila, D. A., 2014, Collisional zones in Puerto Rico and Northern Caribbean: Journal of South America 54, p. 1-19.

Laó-Dávila, D. A., Llerandi-Román P. A., Anderson T. H., 2012, Cretaceous-Paleogene thrust emplacement in southwestern Puerto Rico: GSA Bulletin, 124, p 1169-1190.

Larue, D.K., Pierce, P., and Erickson, J., 1991, Cretaceous intra-Arc summit basin on Puerto Rico, in Gillezeau, K.A., ed., Transactions of the Second Geological Conference of the Geological Society of Trinidad & Tobago, Geological Society of Trinidad and Tobago, p. 184-190.

Llerandi-Román, P.,A., 2004, The Geology of the western section of the Sabana Grande quadrangle: implications for the geological evolution of the southwestern Puerto Rico, [M.A thesis]: University of Puerto Rico Mayagüez Campus

McCann, W.R., 1985, On the earthquake hazard of Puerto Rico and the Virgin Island: Bulletin of the Seismological Society of America, v.75, p. 251-262.

McCann, W. R., 2002, Microearthquake data elucidate details of the Caribbean subduction zone: Seismological Research Letter, v., 73 p. 25-32.

Manaker, D. M., E. Calais, A. M. Freed, S. T. Ali, P. Przybylski, G. Mattioli, P. Jansma, C. Prepetit, and J. B. deChabalier, 2008, Interseismic plate coupling and strain

partioning in the northeastern Caribbean: Geophysical Journal Int., 174, 889–903, doi:10.1111/j.1365-246X.2008.03819.x.

Mann, P., 2005 Introduction, in Mann, P., ed., 2005 Active Tectonics and seismic hazards of Puerto Rico, Virgen Island, and offshore areas: Geological Society of America Special Papers 385, p. 1-12.

Mann, P., Burke, K., 1984, Neotectonics of Hispaniola – Plate motion, sedimentation, and seismicity at a restraining bed: Earth and Planetary Science Letters, no. 70, p. 311-324.

Mann, P., Prentice, C. S., Burr, G., Peña, L R., and Taylor, F. W., 1998, Tectonic geomorphology and paleoseismology of the Septentrional fault system, Dominican Republic, in Dolan, J. F., and Mann, P., eds., Active Strike-slip and Collisional Tectonics 12of the Northern Caribbean Plate Boundary Zone: Boulder, Colorado, Geological Society of America Special Paper 326, p. 63-123.

Mann, P., Prentice, C.S., Hippolyte, J.C., Grindlay, N.R., Abrams, L.J., and Lao-Dávila, D., 2005, Recconnaissance study of Late Quaternary faulting along Cerro Goden fault zone, western Puerto Rico, in Mann, P., ed., Active Tectonics and seismic hazards of Puerto Rico, Virgen Island, and offshore areas: Geological Society of America Special Papers 385, p. 115-138.

Masson, D., G., and Scanlon K., M., 1991, The neotectonics setting of Puerto Rico: Geological Society of America Bulletin, no. 103, p. 144-154.

Mattson, P.H., 1960, Geology of Mayaguez area, Puerto Rico. Geological Society American Bulletin, no. 7 p. 319-362.

Mattson, P. H., 1979. Subduction, Buoyant Braking, Flipping, and Strike-Slip Faulting in the Northern Caribbean: The Journal of Geology, no. 87, p. 293–304.

Mattson, P. H., and Pessagno, 1979. Cretaceous and lower Tertiary stratigraphy in west-central Puerto Rico: U.S. Geological Survey Bulletin 1254-B, 35p.

McIntyre, D.H., 1971, Geologic Map of the Central la Plata Quadrangle, Puerto Rico: U.S. Geological Survey Miscellaneous Investigations Series Map I-660, scale 1:20,000.

Monroe, W., 1973, Stratigraphy and petroleum possibilities of middle Tertiary rocks in Puerto Rico: Bulletin of the American Association of Petroleum Geologists, v. 57, p. 487-494.

Monroe, W., 1976, The Karst landforms of Puerto Rico: U.S. Geological Survey Professional Paper 889.

Monroe, W., 1980, Geology of the middle Tertiary formations of Puerto Rico: U.S. Geological Survey Professional Paper 953, 93.

Montgomery, D.R., Brandon, M.T., 2002. Topographic controls on erosion rates in tectonically active mountain ranges. Earth Planet. Sci. Lett. 201, 481–489.

Motazedian, D., and Atkinson, G., 2005, Ground motion relations for Puerto Rico, in Mann, P., ed., Active Tectonics and seismic hazards of Puerto Rico, Virgen Island, and offshore areas: Geological Society of America Special Papers no. 385, p. 61-80.

Mudd, S., L., Attal, M., Milodowski, D., T., Grieve, S. W. D., Valters D., A., A statistical framework to quantify spatial variation in channel gradients using the integral

method of channel profile analysis: Journal of Geophysical Research Earth Surface, no. 2, p., 138-152.

Pérez-Peña et al., 2010, Active tectonics in the Sierra Nevada (Beltic Cordillera, SE Spain): Insights from geomorphic indexes and drainage patterns analysis: Geomorphology 119, p.74-87.

Perron, J., T., Royden, L., 2013, An integral approach to bedrock river profile analysis: Earh Surface Processes Landforms, no. 6, p. 570-576.

Piety, L., Redwine, J., Derouin S., Prentice C., Kelson, K., Klinger R., and Mahan S., 2018, Holocene Surface Ruptures on the Salinas Fault and Southeastern Great Southern Puerto Rico Fault Zone, South Coastal Plain of Puerto Rico: Bulletin of Seismological Society of America.

Prentice, C., Mann, P., Peña L., and Burr, G., 2003, Slip rate and earthquake recurrence along the central Septentrional fault, North America-Caribbean plate boundary, Dominican Republic: Journal of Geophysical Research, v. 108(B3), 2149.

Prentice, C.S., and Mann, P., 2005, Paleoseismicity study of the South Lajas fault: First documentation of an omshore Holocene fault in Puerto Rico, in Mann, P., ed., Active Tectonics and seismic hazards of Puerto Rico, Virgen Island, and offshore areas: Geological Society of America Special Papers 385, p. 215-222.

Ries, W., F., Location of Active Faults using Geomorphic Indexes in Eroded Landscapes, South Tanaraki, New Zeland, [M.A. thesis]: Victoria University of Wellington, Wellinton, 169 p.

Rodríguez M., O., Barba D., C., and Escribano, D., N., 2017. Morphotectonic Study of the Greater Antilles: Geotectonics, no. 1 pp. 89-104.

Roig-Silva, C., M., Asencio, E., Joyce, J., 2013, The Northwest Trending North Boquerón Bay-Punta Montala Fault Zone; Through Going Active Fault System in Southwestern Puerto Rico: Seismological Research Letter, no. 84, p. 538-550.

Schumm, S.A., Dumont, J.F., Holbrook, J.M., 2002. Active Tectonics and Alluvial Rivers. Cambridge University Press, 276.

Schwanghart, W., and D. Scherler D., 2014, Short Communication: TopoToolbox 2 – MATLAB-based software for topographic analysis and modeling in Earth surface sciences: Earth Surface Dynamics. No.2 p. 1-7.

Slodowski, T.R., 1956, Geology of the Yauco Area, Puerto Rico [Ph.D. thesis]: Princeton, New Jersey, Princeton University, 130 p.

Stein, S., DeMets, C., Gordon, R. G., Brodholt, J., Argus, D., Engeln, J. F., Lundgren, P., Stein, C., Wiens, D. A., and Woods, D, F., 1988, A test of alternaive Caribbean Plate relative motion models: Journal of Geophysical Research, v. 93, p. 3041-3050.

Sykes L., McCann, W., and Kafka, A., 1982, Motion of Caribbean Plate during last seven million years and implications for eartlier Cenozoic movements: Journal of Geophysical Research, v. 87, p. 10,656-10,676.

Symithe., S., Calais, E., Chabalier, J., B., Robertson, R., Higgins, M., 2015, Current block motions and strains accumulation active faults in the Caribbean: no., 120, p. 3748-3774.

Ten Brink and Alberto M. López-Venegas Plate interaction in the NE Caribbean subduction zone from continuous GPS observations, 2012, Geophysical Research Letters, vol. 39, p. L10304.

Volckman, R., P., 1984a, Geologic Map of the Cabo Rojo and Parguera quadrangle Southwest Puerto Rico: U. S. Geological Survey Miscellaneous Investigations Series Map I-1557, scale 1:20,000.

Volckman, R., P., 1984b, Geologic Map of the San Germán quadrangle Southwest Puerto Rico: U. S. Geological Survey Miscellaneous Investigations Series Map I-1558, scale 1:20,000.

Willet, S., D., McCoy, S., Perron, T., Goren, L., Chen, C., Y., 2014, Dynamic Reorganization of River Basins: Science 343 (3175), 1248765.

Wobus, C., Whipple, K., X., Kirby, E., Snyder, N., Johnson, J., Spyropolou, K., Crosby, B., Sheehan, D., 2006, Tectonics from topography: procedures, promises and pitfalls: Geological Society of America Special Papers no. 398, p. 55-74.

Xue, L., Gani, N., Abdelsalam M., 2017, Geomorphic proxies for bedrock rivers: A case study from Rwenzori Mountains Dinamycs: East African Rift System, Geomorphology.

Xue, L., Alemu, T., Gani., N, Abelsalam M., 2018, Spatial and temporal variation of tectonic uplift in the southeastern Ethiopian Plateau from morphotectonic analysis, Geomorphology.

VITA

Type Inés María Barrios Galíndez

Candidate for the Degree of

Master of Science

Thesis: EVALUATION OF GEOMORPHIC PROXIES FROM HIGH RESOLUTION TOPOGRAPHIC DEMs IN OBLIQUE SUBDUCTION ZONES: WESTERN PUERTO RICO

Major Field: Geology

Biographical:

Education:

Completed the requirements for the Master of Science in your major at Oklahoma State University, Stillwater, Oklahoma in May.

Completed the requirements for the Bachelor of Science in your major at Carabobo University, Valencia, Carabobo/Venezuela in 2007.

Experience:

I worked for five years in the Venezuelan construction industry focused on project engineering. Currently, I am on my second year of master in geology at Oklahoma State University. I am conducting research on active tectonics in Western Puerto Rico. During my master's experience, I have participated as part of the OSU team in the Imperial Barrel Award by AAPG because of my interest in Oil and Gas exploration. In addition, I enjoyed class projects related to gravity and magnetic exploration and study abroad to explore Puerto Rico and Caribbean geology.

Professional Memberships:

American Association of Petroleum Geologist (AAPG)
Society of Exploration Geophysisists (SEG)
American Geophysical Union (AGU)
Geological Society of America (GSA)
Oklahoma City Geological Society (OCGS)